Azhdarchid pterosaur diversity in the Bayanshiree Formation, Upper Cretaceous of the Gobi Desert, Mongolia (#112610)

First submission

Guidance from your Editor

Please submit by **13 May 2025** for the benefit of the authors (and your token reward) .

Structure and Criteria
Please read the 'Structure and Criteria' page for guidance.

Custom checks
Make sure you include the custom checks shown below, in your review.

Author notes
Have you read the author notes on the guidance page?

Raw data check
Review the raw data.

Image check
Check that figures and images have not been inappropriately manipulated.

If this article is published your review will be made public. You can choose whether to sign your review. If uploading a PDF please remove any identifiable information (if you want to remain anonymous).

Files

Download and review all files from the materials page.

7 Figure file(s)
1 Table file(s)
3 Other file(s)

Custom checks

New species checks

- Have you checked our new species policies?
- Do you agree that it is a new species?
- Is it correctly described e.g. meets ICZN standard?

Structure and Criteria

Structure your review

The review form is divided into 5 sections. Please consider these when composing your review:

1. **BASIC REPORTING**
2. **EXPERIMENTAL DESIGN**
3. **VALIDITY OF THE FINDINGS**
4. General comments
5. Confidential notes to the editor

You can also annotate this PDF and upload it as part of your review

When ready submit online.

Editorial Criteria

Use these criteria points to structure your review. The full detailed editorial criteria is on your guidance page.

BASIC REPORTING

- Clear, unambiguous, professional English language used throughout.
- Intro & background to show context. Literature well referenced & relevant.
- Structure conforms to PeerJ standards, discipline norm, or improved for clarity.
- Figures are relevant, high quality, well labelled & described.
- Raw data supplied (see PeerJ policy).

EXPERIMENTAL DESIGN

- Original primary research within Scope of the journal.
- Research question well defined, relevant & meaningful. It is stated how the research fills an identified knowledge gap.
- Rigorous investigation performed to a high technical & ethical standard.
- Methods described with sufficient detail & information to replicate.

VALIDITY OF THE FINDINGS

- **Impact and novelty is not assessed.** Meaningful replication encouraged where rationale & benefit to literature is clearly stated.
- All underlying data have been provided; they are robust, statistically sound, & controlled.
- Conclusions are well stated, linked to original research question & limited to supporting results.

Standout reviewing tips

The best reviewers use these techniques

Tip	*Example*
Support criticisms with evidence from the text or from other sources	*Smith et al (J of Methodology, 2005, V3, pp 123) have shown that the analysis you use in Lines 241-250 is not the most appropriate for this situation. Please explain why you used this method.*
Give specific suggestions on how to improve the manuscript	*Your introduction needs more detail. I suggest that you improve the description at lines 57- 86 to provide more justification for your study (specifically, you should expand upon the knowledge gap being filled).*
Comment on language and grammar issues	*The English language should be improved to ensure that an international audience can clearly understand your text. Some examples where the language could be improved include lines 23, 77, 121, 128 – the current phrasing makes comprehension difficult. I suggest you have a colleague who is proficient in English and familiar with the subject matter review your manuscript, or contact a professional editing service.*
Organize by importance of the issues, and number your points	*1. Your most important issue* *2. The next most important item* *3. …* *4. The least important points*
Please provide constructive criticism, and avoid personal opinions	*I thank you for providing the raw data, however your supplemental files need more descriptive metadata identifiers to be useful to future readers. Although your results are compelling, the data analysis should be improved in the following ways: AA, BB, CC*
Comment on strengths (as well as weaknesses) of the manuscript	*I commend the authors for their extensive data set, compiled over many years of detailed fieldwork. In addition, the manuscript is clearly written in professional, unambiguous language. If there is a weakness, it is in the statistical analysis (as I have noted above) which should be improved upon before Acceptance.*

Azhdarchid pterosaur diversity in the Bayanshiree Formation, Upper Cretaceous of the Gobi Desert, Mongolia

Rodrigo Vargas Pêgas [1], **Xuanyu Zhou** [Corresp., 2], **Yoshitsugu Kobayashi** [3]

[1] Museu de Zoologia da USP, São Paulo, Brazil

[2] Shihezi University, Shihezi, China

[3] Hokkaido University, Sapporo, Japan

Corresponding Author: Xuanyu Zhou
Email address: xyzhou@elms.hokudai.ac.jp

Pterosaur remains are very rare in Mongolian Mesozoic deposits, in stark contrast with the great abundance of dinosaur fossils. This contribution presents a reassessment of the azhdarchid pterosaur remains from the Bayanshiree Formation's "upper beds" (Turonian–Santonian), represented by two specimens coming from two distinct localities: the Burkhant and the Bayshin Tsav azhdarchids. These specimens, collected by the Japanese−Mongolian Joint Paleontological Expedition and originally described in 2009, have been previously interpreted as indeterminate azhdarchids. Under the light of current knowledge on the morphological diversity of azhdarchid cervical vertebrae, as well as on the taxonomic and phylogenetic signals these skeletal elements carry, we herein identify diagnostic features and reassess the phylogenetic affinities of the Bayanshiree azhdarchids in further detail. Our results suggest that the Burkhant azhdarchid, hereby named *Gobiazhdarcho tsogtbaatari* gen. et sp. nov., represents a medium-sized (3.0–3.5 meters in wingspan) basal member of a *Quetzalcoatlus-Arambourgiania* lineage. The Bayshin Tsav azhdarchid, *Tsogtopteryx mongoliensis* gen. et sp. nov., is recovered as a basal member of a *Hatzegopteryx*-lineage and, surprisingly, seems to represent a small form under 2 m in wingspan. Our results shed fresh light on the diversity and phylogeny of azhdarchid pterosaurs, and reinforce the reoccurring pattern of coexistence between multiple, differently-sized azhdarchid species in a same deposit.

Azhdarchid pterosaur diversity in the Bayanshiree Formation, Upper Cretaceous of the Gobi Desert, Mongolia

Rodrigo V. Pêgas[1], Xuanyu Zhou[2*], Yoshitsugu Kobayashi[3]

1. Zoology Museum, São Paulo University, Avenida Nazaré 481, 04263-000, São Paulo, SP, Brazil.

2. College of Life Sciences, Shihezi University, Shihezi, Xinjiang, China.

3. Hokkaido University Museum, Hokkaido University, Sapporo, Japan.

Corresponding Author:

Xuanyu Zhou

Shihezi University, Shihezi, China

Email address: zhou.xuanyu@shzu.edu.cn

Abstract

Pterosaur remains are very rare in Mongolian Mesozoic deposits, in stark contrast with the great abundance of dinosaur fossils. This contribution presents a reassessment of the azhdarchid pterosaur remains from the Bayanshiree Formation's "upper beds" (Turonian–Santonian), represented by two specimens coming from two distinct localities: the Burkhant and the Bayshin Tsav azhdarchids. These specimens, collected by the Japanese-Mongolian Joint Paleontological Expedition and originally described in 2009, have been previously interpreted as indeterminate azhdarchids. Under the light of current knowledge on the morphological diversity of azhdarchid cervical vertebrae, as well as on the taxonomic and phylogenetic signals these skeletal elements carry, we herein identify diagnostic features and reassess the phylogenetic affinities of the Bayanshiree azhdarchids in further detail. Our results suggest that the Burkhant azhdarchid, hereby named *Gobiazhdarcho tsogtbaatari* gen. et sp. nov., represents a medium-sized (3.0–3.5 meters in wingspan) basal member of a *Quetzalcoatlus-Arambourgiania* lineage. The Bayshin Tsav azhdarchid, *Tsogtopteryx mongoliensis* gen. et sp. nov., is recovered as a basal member of a *Hatzegopteryx*-lineage and, surprisingly, seems to represent a small form under 2 m in wingspan. Our results shed fresh light on the diversity and phylogeny of azhdarchid pterosaurs, and reinforce the reoccurring pattern of coexistence between multiple, differently-sized azhdarchid species from a same deposit.

Introduction

Pterosaurs, the first vertebrate group to evolve powered flight, exhibit a fossil record stretching from the Late Triassic to the Cretaceous/Paleogene boundary, and an impressive diversity (Wellnhofer, 1991; Witton, 2013; Jagielska & Brusatte, 2021). Within pterosaurs, Azhdarchidae represents a very particular clade. Characterized mainly by their elongate cervical vertebrae with vestigial neural spines, azhdarchids are an almost ubiquitous presence in Turonian–Maastrichtian pterosaur assemblages worldwide, being the most diverse and widespread group of pterosaurs

during the Late Cretaceous (Longrich *et al.*, 2018; Andres, 2021). Similar to other azhdarchoids, azhdarchids sported edentulous jaws and seem to have been relatively terrestrial in lifestyle compared to other pterosaurs (see Witton & Naish, 2008; Witton & Habib, 2010; Witton, 2013). At present, the group counts with at least 16 nominal species (see Andres, 2021; Ortiz-David *et al.*, 2022; Zhou *et al.*, 2024). Azhdarchids are well-known especially for including the largest flying creatures ever, comprising some gigantic forms with 10–11 meter-wingspans such as *Quetzalcoatlus northropi*, *Arambourgiania philadelphiae*, and *Hatzegopteryx thambema* (see Witton & Habib, 2010; Andres & Langston, 2021), as well as the ~9 meter-wingspan *Thanatosdrakon amaru* (Ortiz-David *et al.*, 2022). The group also includes smaller forms such as the 4.5 meter-wingspan *Quetzalcoatlus lawsoni* (Andres & Langston, 2021), the 3.5 meter-wingspan *Zhejiangopterus linhaiensis* (Cai & Wei, 1994), the 3.0 meter-wingspan *Eurazhdarcho langendorfensis* (Vremir *et al.*, 2013), and, potentially, the ~1.6 meter-wingspan Hornby pterosaur (Martin-Silverstone *et al.*, 2016).

Mesozoic deposits in Mongolia, especially in the Gobi Desert, are well-known for their rich fossil record (particularly regarding dinosaurs), what results from an outstanding history of paleontological expeditions in the country (e.g. Andrews, 1932; Rozhdestvenskii, 1960; Kielan-Jaworowska, 1969; Lavas, 1993; Novacek, 1996; Colbert, 2000; Kurochkin & Barsbold, 2000; Watabe *et al.*, 2000; 2010). Still, in stark contrast to dinosaurs, the Mongolian record of pterosaurs is exceedingly scarce (Watabe *et al.*, 2009; Tsuihiji *et al.*, 2017). The most notable example is *Noripterus parvus*, which is so far the only nominal species of pterosaur from Mongolia (Bakhurina, 1982). This taxon is represented by several remains from the latest Jurassic–Early Cretaceous Tsagan-Tsab Formation of Western Mongolia (see Bakhurina, 1982; 1986; Lü *et al.*, 2009). The Mongolian pterosaur record only includes seven further specimens: an undescribed anurognathid from the Middle Jurassic beds of Bakhar in Central Mongolia (Bakhurina & Unwin, 1995), a tapejaroid cervical vertebra from the Öösh Formation (Andres & Norell, 2005), an undescribed anhanguerid from the Albian Khuren Dukh Formation (Bakhurina & Unwin, 1995), two fragmentary azhdarchid specimens from the Late Cretaceous Bayanshiree Formation (Watabe *et al.*, 2009), a fragmentary ?azhdarchid long bone preserved as gut content of a dromaeosaurid specimen from the Tugrikin Shireh beds (Hone *et al.*, 2012), and fragmentary remains of a giant azhdarchid from the Maastrichtian Nemegt Formation (Tsuihiji *et al.*, 2017). Only the last four findings come from the Gobi Desert (Bakhurina & Unwin, 1995;

Watabe *et al.*, 2009; Tsuihiji *et al.*, 2017). Further pterosaur remains from the Gobi Desert include only some isolated bones from the Late Cretaceous Iren Dabasu Formation in Inner Mongolia, China (Currie & Eberth, 1993), attesting the rarity of pterosaur remains in the Gobi region (perhaps linked to paleoecological factors; see Averianov, 2014).

The Bayanshiree azhdarchids comprise two specimens: the Bayshin Tsav azhdarchid, comprising an almost complete mid-cervical; and the Burkhant azhdarchid, comprising an atlantoaxis, a cervical III, and a partial mid-cervical (Watabe *et al.*, 2009). These specimens were collected by the *Hayashibara Museum of Natural Sciences-Mongolian Paleontological Center Joint Paleontological Expedition* in 1993 and 1995 from, respectively, the Bayshin Tsav and Burkhant localities (Watabe *et al.*, 2009). These remains were originally described in detail by Watabe *et al.* (2009) and interpreted as indeterminate azhdarchids.

The present paper aims at redescribing these specimens and investigating their phylogenetic relationships within Azhdarchidae, under the light of present-day data concerning azhdarchid diversity. This topic that has been the subject of many studies and great developments lately, and the taxonomic usefulness of cervical vertebrae morphology has become increasingly evident for azhdarchids (Vremir *et al.*, 2015; Witton & Naish, 2017; Longrich *et al.*, 2018; Pêgas *et al.*, 2021; Andres, 2021; Andres & Langston, 2021; Zhou *et al.*, 2024).

Material & Methods

Geological setting

The Bayanshiree Formation (also spelled Bayan Shireh, Baynshire, Bayshiree, or Baysheen Shireh Formation) is located in the eastern region of the Gobi Desert, in Mongolia. It can be divided in two members, informally dubbed as “upper” and “lower” beds (Jerzykiewicz & Russell, 1991; Averianov & Sues, 2012). The Bayanshiree Formation consists mostly of mudstones and sandstones, deposited in lacustrine to fluvial systems in a semi-arid paleoenvironment (Shuvalov, 2000; Watabe *et al.*, 2009; 2010).

The paleontological record of the Bayanshiree Formation is relatively rich, with a flourishing dinosaur fauna that includes ankylosaurids, pachycephalosaurids, ceratopsians,

hadrosauroids, sauropods, and theropods (e.g. Benton *et al.*, 2000; Watabe *et al.*, 2000; 2011; Barsbold *et al.*, 2007; Tsogtbaatar *et al.*, 2019). Notoriously, the turtle fauna is also very diverse, with numerous remains representing about 8 species (Danilov *et al.*, 2014). Mesozoic mammals (Rougier *et al.*, 2015; Lopatin & Averianov, 2023) and crocodylians (Turner, 2015) also occur. Pterosaur remains are very rare, and limited to the two specimens previously described by Watabe *et al.* (2009) and herein redescribed. As mentioned above, these pterosaur specimens come from outcrops of the Burkhant and Bayshin Tsav localities, both of which lie within the "upper beds" (Averianov & Sues, 2012).

Burkhant and Bayshin Tsav are well-known fossiliferous localities (Fig. 1), having been extensively explored on the literature before. The Burkhant locality (Dornogovi Province) is the same site that has yielded the holotype of the large dromaeosaurid theropod *Achillobator giganticus* (Perle *et al.*, 1999), while the Bayshin Tsav locality (Ömnögovi Province) has yielded remains of the ornithomimosaur *Garudimimus brevipes* (Kobayashi & Barsbold, 2005), the therizinosaurids *Erlikosaurus andrewsi* and *Segnosaurus galbinensis* (Perle, 1979; 1981; Barsbold & Perle 1983; Zanno, 2010), the ankylosaurid *Talarurus plicatospineus* (Park *et al.*, 2020), and the hadrosaurid *Gobihadros mongoliensis* (Tsogtbaatar *et al.*, 2019).

The age of the Bayanshiree Formation has been the subject of several studies, and conclusions mostly converge towards a Cenomanian–Santonian age, summarized as follows. Paleomagnetic analyses have indicated that the upper levels of the formation do not cross the Santonian–Campanian interval, meaning the upper limit of the Bayanshiree Formation is no younger than the latest Santonian (Hicks *et al.*, 1999). Biostratigraphic analyses of the mollusk assemblages of the upper levels of the formation also suggest a Coniacian–Santonian upper limit (Martinson, 1975; 1982). More recently, direct dating using calcite U-Pb measurements (taken from caliche samples) have indicated an age between 95.9 ± 6.0 and 89.6 ± 4.0 Ma, suggesting the Bayanshiree Formation lies somewhere within the Albian–Santonian interval (Kurumada *et al.*, 2020). However, an age no older than the Cenomanian is indicated by both palynological and paleomagnetic evidence (Hicks *et al.*, 1999; Shuvalov, 2000). Taken together, all of this data suggest that the Bayanshiree Formation is most likely Cenomanian–Santonian in age, as usually accepted (Shuvalov, 2000). Based on vertebrate faunal correlations, it has been suggested that the "lower beds" of the Bayanshiree Formation are Cenomanian–late Turonian in age, while the

"upper beds" are late Turonian–Santonian in age (Averianov & Sues, 2012; Danilov *et al.*, 2014).

Anatomical terminology

The present work largely follows the anatomical terminologies provided by Andres & Langston (2021). As such, we restrict the term 'preexapophysis' for the distinct process on the ventral surface of the prezygapophyseal pedicle (when present), as opposed to the 'preexapophyseal articulation' which is continuous with the cotylar surface (Bennett, 2001; Andres & Langston, 2021). Following Andres & Langston (2021), we use the terms 'mid-cervical' for cervicals IV-VI, and 'middle-series cervicals' for cervicals III-VII. In this sense, we further suggest here the use of the term 'mesocervical' as a synonym for 'middle-series cervical', for brevity. We further adopt the terms 'accessory foramen' and 'adjacent foramen' for the pneumatic foramina located, respectively, dorsal and lateral to the neural canal (Hone *et al.*, 2019). Other anatomical terms are the same as in the work of Andres & Langston (2021).

Phylogenetic analysis

A phylogenetic analysis was performed in order to investigate the relationships of the new species herein analyzed within Azhdarchidae. For this purpose, we have utilized as a basis the phylogenetic matrix of Zhou *et al.* (2024). As in Pêgas (2024), the character list derives from a comprehensive survey of the literature (Howse, 1986; Bennett, 1994; Kellner, 2003; 2004; Unwin, 2003; Dalla Vecchia, 2009; 2019; Lü *et al.*, 2009; Wang *et al.*, 2012; Naish *et al.*, 2013; Andres *et al.*, 2014; Pêgas *et al.*, 2016; 2018; 2019; 2021; 2023; Vidovic & Martill, 2017; Longrich *et al.*, 2018; Holgado *et al.*, 2019; Kellner *et al.*, 2019; Zhou *et al.*, 2019; 2021; Andres, 2021).

The analysis was conducted under maximum parsimony, using the software TNT 1.5 (Goloboff *et al.*, 2016). The analysis was divided in two steps, following the same protocol as previously described by Wei *et al.* (2020). New Technology Search was used for the first step (using Sectorial Search, Ratchet, Drift and Tree fusing, default parameters), with random seed =

0. Subsequently, a Traditional Search swapping was performed using trees from RAM (using TBR, 10000 replications, collapsing trees after search). All characters were treated with equal weights. A Mesquite file (Nexus format) containing the data matrix and a TNT file, ready for analysis execution in TNT, are available as Supplemental Files 1 and 2, respectively.

As many of our characters/states pertain to cervical anatomy, care was taken to avoid characters affected by serial variation, taking the cervical series of *Q. lawsoni* and *W. brevirostris* as comparative bases. Azhdarchid species circumscriptions and coding sources are outlined below.

Azhdarchid species circumscriptions

Here we follow Vremir *et al.* (2015) in considering that isolated, non-overlapping azhdarchid remains coming from a same deposit should be seen with caution, as the presence of multiple azhdarchid species in a same deposit seems to be a common, reoccurring condition. This can be seen, for example, in the Haţeg Basin (Vremir *et al.*, 2015; Solomon *et al.*, 2019), the Ouled Abdoun Basin (Longrich *et al.*, 2018), and the Javelina Formation (Andres & Langston, 2021). For this reason, we regard that species circumscriptions for the taxa *Azhdarcho lancicollis*, *Aralazhdarcho bostobensis*, and *Cryodrakon boreas* require detailed revisions. Regarding *Azhdarcho lancicollis*, we note here that it autapomorphically exhibits a strongly sinusoidal medial margin of the prezygapophyseal peduncle, as can be seen in its type-specimen (Averianov, 2010). We herein provisionally restrict the circumscription of *Azhdarcho lancicollis* to specimens in which this same feature can be seen, such as ZIN PH 131/44 and ZIN PH 147/44 (see Averianov, 2010). Other referred specimens should be seen with caution, as Azhdarchidae indet. Similarly, the circumscription of *Cryodrakon boreas* is herein provisionally restricted to its holotype plus the two specimens that unambiguously exhibit some of its autapomorphic features, TMP 1993.40.11 and TMP 1989.36.254 (see Hone *et al.*, 2019), with other specimens being herein regarded as Azhdarchidae indet. Regarding *Aralazhdarcho bostobensis*, its circumscription is herein provisionally restricted to its holotype. We further follow Longrich *et al.* (2018) for the circumscription of *Phosphatodraco mauritanicus*; Andres & Langston (2021) for the Javelina Fm. azhdarchids; Vremir (2010) and Naish & Witton (2017) for *Hatzegopteryx*

thambema; and Frey & Martill (1996) and Martill & Moser (2018) for *Arambourgiania philadelphiae*.

Phylogenetic nomenclature

The present work follows the PhyloCode (de Queiroz & Cantino, 2020) as a means of standardizing phylogenetic nomenclature. We primarily follow the phylogenetic definitions of Andres (2021) along with the updates of Pêgas *et al.* (2021) concerning azhdarchids. The phylogenetic nomenclatural scheme employed here, following recommendations of the PhyloCode (de Queiroz *et al.*, 2020), is presented in Table 1.

Nomenclatural acts

The electronic version of this article in Portable Document Format (PDF) will represent a published work according to the International Commission on Zoological Nomenclature (ICZN), and hence the new names contained in the electronic version are effectively published under that Code from the electronic edition alone. This published work and the nomenclatural acts it contains have been registered in ZooBank, the online registration system for the ICZN. The ZooBank LSIDs (Life Science Identifiers) can be resolved and the associated information viewed through any standard web browser by appending the LSID to the prefix http://zoobank.org/. The LSID for this publication is urn:lsid:zoobank.org:pub:72240BB4-B98C-40B4-ADBC-A1DEDE9E06DA. The LSID for the new genus *Gobiazhdarcho* is: urn:lsid:zoobank.org:act:A675EB7D-3502-4F99-8446-8AE4918AC60A. The LSID for the species *Gobiazhdarcho tsogtbaatari* is: urn:lsid:zoobank.org:act:59F3DABA-6E84-4DE2-8948-F5F250E2E910. The LSID for the new genus *Tsogtopteryx* is: urn:lsid:zoobank.org:act:A724E4E3-A6EA-415E-9A12-0B8F0636FEF0. The LSID for the species *Tsogtopteryx mongoliensis* is: urn:lsid:zoobank.org:act:3F218EE5-2CB8-469D-A252-C5194C7C6911.

Institutional abbreviations

EME, Transylvanian Museum Society, Cluj-Napoca, Romania; **FSAC**, Faculté des Sciences Aïn-Chock, Université Hassan II, Casablanca, Morocco; **LPB**, Laboratory of Fossil Vertebrates, Faculty of Geology and Geophysics, University of Bucharest, Bucharest, Romania; **MPC**, Mongolian Paleontological Center, Mongolian Academy of Sciences, Ulaanbaatar, Mongolia; **SNSB-BSPG**, Staatliche Naturwissenschaftliche Sammlungen Bayerns/Bayerische Staatssammlung für Palaontologie und Geologie, Munich, Germany; **TMM**; Texas Vertebrate Paleontology Collections, The University of Texas at Austin, Austin, Texas; **TMP**, Royal Tyrrell Museum of Palaeontology, Drumheller, Alberta, Canada; **ZMNH**, Zhejiang Museum of Natural History, Hangzhou, China; **ZIN**, Zoological Institute of the Russian Academy of Sciences, St. Petersburg, Russia.

Materials Availability

The two specimens herein redescribed are permanently stored at the Mongolian Paleontological Center (Mongolian Academy of Sciences, Ulaanbaatar, Mongolia), a public research institution and repository, where the specimens are available for research upon request. Specimen ID's are MPC−Nd 100/302 (the Burkhant azhdarchid; *Gobiazhdarcho tsogtbaatari* gen. et sp. nov.) and MPC−Nd 100/303 (the Bayshin Tsav azhdarchid; *Tsogtopteryx mongoliensis* gen. et sp. nov.). Furthermore, the dataset associated with our phylogenetic analysis is available as Supplemental Files 1 (Nexus format) and 2 (TNT format).

Systematic Paleontology

Pterosauria Owen, 1842 *sensu* [Andres & Padian, 2020a]

Pterodactyloidea Plieninger, 1901 *sensu* [Andres & Padian, 2020b]

Azhdarchoidea Unwin, 1995 *sensu* [Andres, 2021]

Azhdarchidae Padian, 1986 *sensu* {this work}

Definition (unrestricted emendation). The least inclusive clade containing *Azhdarcho lancicollis* Nessov 1984, *Phosphatodraco mauritanicus* Pereda-Suberbiola *et al.* 2003,

Zhejiangopterus linhaiensis Cai & Wei 1994, and *Quetzalcoatlus northropi* Lawson 1975. RegNum registration number: {1043}. This is an unrestricted emendation (original definition: Andres, 2021).

Composition. *Aerotitan sudamericanus*, *Aralazhdarcho bostobensis*, *Azhdarcho lancicollis*, *Eurazhdarcho langendorfensis*, *Mistralazhdarcho maggi*, *Phosphatodraco mauritanicus*, *Wellnhopterus brevirostris*, *Zhejiangopterus linhaiensis*, and Quetzalcoatlida (see below).

Diagnostic apomorphies. Mesocervical vertebrae neural spines vestigial (composed of anterior and posterior neural processes, connected by a neural ridge); mid-cervical vertebrae extremely elongated (maximum length/width ratio over 5); wing digit phalanges 2 and 3 bearing a ventral keel.

Remarks. Azhdarchids have traditionally and consistently been diagnosed by their unique cervical osteology, most notably characterized by extremely elongated vertebrae with vestigial neural spines (Padian, 1986; Kellner, 2003; Unwin, 2003; Andres, 2021). When originally defined in accordance with the PhyloCode, this clade reflected such traditional and consistent usage, at least under the context of the original definitional reference phylogeny (Andres, 2021). Azhdarchidae was then defined as the least inclusive clade containing *Azhdarcho lancicollis* and *Quetzalcoatlus northropi* (Andres, 2021). In this sense, azhdarchids *sensu* Andres (2021) share the following apomorphies: middle-series cervical vertebrae maximum length/width ratio over 4.8; middle-series cervical neural spines vestigial; and wing digit phalanges 2 and 3 bearing a ventral keel; and comprise the same nominal species as in here (with the addition of *Thanatosdrakon amaru* and *Nipponopterus mifunensis* here, as well as the herein named taxa).

As regulated by the PhyloCode (de Queiroz & Cantino, 2020), an unrestricted emendation is "*a mechanism to prevent undesirable changes in the application of a particular name (in terms of clade conceptualization) when the original definition is applied in the context of a revised phylogeny*" (Article 15.11). This is the case here, where direct application of the original definition would leave a large number of taxa consistently and universally included in Azhdarchidae outside of the group; thereby severely disrupting not only the composition of Azhdarchidae but also its diagnosis. Therefore, fulfilling Article 15 of the PhyloCode and aiming at preserving the clade's original diagnosis and composition under the context of the present phylogeny, an unrestricted emendation is herein proposed. It is worth noting that, for workers

who may prefer alternative phylogenies, the previous definition (Andres, 2021) will still take precedence, following Article 15.15 of the PhyloCode.

Quetzalcoatlida new clade name (Table 1)

Quetzalcoatlini new clade name (Table 1)

Gobiazhdarcho tsogtbaatari gen. et sp. nov.

Holotype. MPC−Nd 100/302 (Figs. 2–4), the Burkhant azhdarchid (Watabe *et al.*, 2009). The specimen includes the atlantoaxis, cervical III, and fragmentary cervical VI (Andres & Langston, 2021).

Etymology. The generic epithet is a combination of the words *Gobi*, in reference to the Gobi Desert, and *azhdarcho* (from Persian *azhdar*, a dragon-like creature), a common suffix for azhdarchid pterosaurs. The specific epithet honors Khishigjav Tsogtbaatar, in recognition of his contributions to Mongolian vertebrate paleontology.

Type locality and horizon. Bluish white siltstone layer, Burkhant locality, Eastern Gobi Aimag (Watabe *et al.*, 2009). Upper Bayanshiree Formation, Turonian–Santonian (see Averianov & Sues, 2012).

Diagnostic apomorphies. Regarding mesocervical vertebrae morphology: prezygapophyseal pedicle with a large ventral tubercle anterior to the preexapophyses; postexapophyses reduced; presence of an interpostexapophyseal lamina; presence of five longitudinal ridges on the ventral surface of the postexapophyses; epipophyses dorsal surface keeled, bearing an acuminated apex; CVI epipophyses strongly curving medially.

Description and comparisons. Even though this specimen has already been explored in detail by Watabe *et al.* (2009), a redescription with complementary details and comparisons is herein presented. The specimen includes three elements: a complete atlantoaxis, a roughly complete cervical III, and a fragmentary cervical VI.

Atlantoaxis. The atlas and axis are fused into an atlantoaxis (Fig. 2), as is typical in Ornithocheiroidea (e.g. Andres, 2021). The fusion is complete, and no clear traces of sutures

could be found. The element is roughly complete, except for some minor damage on the dorsal edge of the neural spine.

Delimitations between atlanteal elements cannot be discerned. The cotyle of the atlas is subcircular in shape (Fig. 2A, D), unlike the piriform (ventrally acuminated) shape found in cf. *Azhdarcho lancicollis* (ZIN PH 105/44; Averianov, 2010) and *Quetzalcoatlus lawsoni* (Andres & Langston, 2021). Above the cotyle, the neural canal is as (laterolaterally) wide as, and (dorsoventrally) lower than, the cotyle, as in both cf. *Azhdarcho lancicollis* (Averianov, 2010) and *Quetzalcoatlus lawsoni* (Andres & Langston, 2021). Still, it differs from both of these forms in that the neural canal opening is relatively more dorsoventrally depressed (roughly semicircular), rather than subtriangular. Ventral to the cotyle, a gentle midline process projecting anteriorly is present (presumably the intercentrum; Fig. 2K); much more discrete than in either cf. *Azhdarcho lancicollis* (Averianov, 2010) or *Quetzalcoatlus lawsoni* (Andres & Langston, 2021). The lateral surface of the atlas is pierced by a distinctive intervertebral foramen, as in cf. *Azhdarcho lancicollis* (Averianov, 2010) and *Quetzalcoatlus lawsoni* (Andres & Langston, 2021). In the Burkhant azhdarchid, this foramen lies ventral to the level of the axis condyle, similar to *Quetzalcoatlus lawsoni* but unlike cf. *Azhdarcho lancicollis*, in which it lies further higher (Averianov, 2010).

The axis lacks any pneumatic foramina (Fig. 2), similar to cf. *Azhdarcho lancicollis* and *Quetzalcoatlus lawsoni* but unlike *Mistralazhdarcho maggi* in which a lateral pneumatic foramen is present (Vullo *et al.*, 2018). The neural spine is reduced (occupying only the first half of the atlantoaxis length) and anteriorly-facing, thus being excluded from the posterodorsal apex of the element (Fig. 2B, C, H). This is similar to the condition seen in *Quetzalcoatlus lawsoni* (Andres & Langston, 2021) though less reduced, and quite distinct from the more typical condition seen in cf. *Azhdarcho lancicollis*, wherein the neural spine forms the posterodorsal apex of the element (Averianov, 2010). The posterior face of the neural arch, above the postzygapophyseal pedicles, bears a pair of well-developed fossae. This feature is absent in cf. *Azhdarcho lancicollis* and *Quetzalcoatlus lawsoni*. The postzygapophyseal pedicles are massively constructed, roughly as dorsoventrally tall as the centrum. The epipophyses are well-developed, as in cf. *Azhdarcho lancicollis* (Averianov, 2010) and *Quetzalcoatlus lawsoni* (Andres & Langston, 2021), but differ from these forms in being dorsally keeled rather than blunt. The posterior neural canal opening is

dorsoventrally elongate and slit-like in shape (Fig. 2G, J), unlike the subcircular conditions seen in cf. *Azhdarcho lancicollis*, *Quetzalcoatlus lawsoni*, and *Mistralazhdarcho maggi*. The condyle is gently cordate (Fig. 2G, J), similar to cf. *Azhdarcho lancicollis* (Averianov, 2010) but unlike the ovoid shape found in *Quetzalcoatlus lawsoni* (Andres & Langston, 2021) and *Mistralazhdarcho maggi* (Vullo *et al.*, 2018).

Cervical III. The third cervical is almost completely preserved (Fig. 3), despite damage on the neural spine and postzygapophyses, the latter of which are mostly missing. It is moderately elongated, with a maximum length/width ratio of 4.4; lower than the same ratio in *Q. lawsoni* (7.4; Andres & Langston, 2021) but similar to *Eurazhdarcho langendorfensis* (~4) and ?*A. lancicollis* (4.38; Averianov, 2010), and slightly higher than in *Phosphatodraco mauritanicus* (~3; Pereda-Suberbiola *et al.*, 2003; Kellner, 2010) and *Zhejiangopterus linhaiensis* (~3; Cai & Wei, 1994). The neural spine is tall, as in all other known azhdarchid third cervicals (Averianov, 2010; Vremir *et al.*, 2013; Andres & Langston, 2021). The neurocentral shaft shows taphonomic distortion caused by an expansion (presumably caused by mineral infiltration or expansion) at the anterior third of its length (Fig. 3A, D). A similar distortion can be seen in *Quetzalcoatlus lawsoni* specimen TMM 41544-15 (Andres & Langston, 2021). Disregarding such distortion, the lateral margins of the vertebra seem to have been gently curved in ventral and dorsal views.

The neural spine is single (not bifid), as typical of azhdarchid third cervicals and unlike azhdarchid mid-cervicals (Andres & Langston, 2021). It extends for almost the entire dorsal surface of the neural arch (Fig. 3A, D), as in *Eurazhdarcho langendorfensis* (Vremir *et al.*, 2013) and cf. *Azhdarcho lancicollis* (ZIN PH 131/44; Averianov, 2010) but unlike *Quetzalcoatlus lawsoni* in which it is more restricted towards the mid-shaft (Andres & Langston, 2021). On the anterior vestibule, it can be seen that the neural canal opening is piriform (Fig. 3C), being mostly subcircular except for a tapered dorsal apex. A pair of adjacent foramina are present. The adjacent foramina are approximately aligned with the center of the neural canal opening. The prezygapophyseal pedicles bear a ventral tubercle just anterior to the preexapophyses on both sides (Fig. 3C, F). The prezygapophyseal articular facets are anteriorly expanded with a squared-off anterior margin, unlike the elliptical shape seen in cf. *Azhdarcho lancicollis* (Averianov, 2010) and *Quetzalcoatlus lawsoni* (Andres & Langston, 2021).

The vertebra exhibits a transverse ridge that is slightly dorsally reflected (Fig. 3A, D), similar to mid-cervicals of *Quetzalcoatlus lawsoni* and *Arambourgiania philadelphiae* (Andres & Langston, 2021). Ventral to this dorsolateral ridge lies a lateral ridge, which extends from the lateral surface of the base of the prezygapophyseal pedicle until the mid-length of the vertebra. As previously noted (Andres & Langston, 2021), the ventral surface produces a ventral tumescence on the anterior region (posterior to a small, blunt hypapophysis) extending posteriorly as a raised band until the mid-length of the vertebrae, giving the anterior half of the ventral margin a convex aspect in lateral view, similar to the third cervicals of *Eurazhdarcho langendorfensis* (Vremir *et al.*, 2013), cf. *Azhdarcho lancicollis* (Averianov, 2010), and *Quetzalcoatlus lawsoni* (Andres & Langston, 2021).

The posterior vestibule houses a clithridiate neural canal (Fig. 3I), which exhibits an incipient (?vestigial) bony bar that almost separates it into neural canal and accessory foramen. A pair of adjacent foramina are present. The postzygapophyses are almost entirely lacking, and so not much can be observed. The condyle is ovoid in shape, with a convex dorsal margin in posterior view. This is similar to the condition seen in ?*Azhdarcho lancicollis* (Avernianov, 2010), but unlike the chordate condition seen in *Quetzalcoatlus lawsoni* (Andres & Langston, 2021). The postexapophyses are quite anteroposteriorly short. The ventral surface of the centrum between the postexapophyses produces a transverse lamina, which connects the two postexapophyses. The ventral surface between the postexapophyses is concave, though not developed into a fossa. Despite superficial damage, it can be seen that a set of five longitudinal ridges are present on this ventral surface (two paired ones plus a median one). A single, median ridge is located on the sagittal line, and a further pair of ridges are located on each postexapophysis.

Cervical VI. The third element, MPC−Nd 100/302c, comprises the posterior region of a mesocervical (Fig. 4). It has been originally interpreted as an indeterminate mesocervical (Watabe *et al.*, 2009), and later reinterpreted as either a cervical IV (Averianov, 2014) or a cervical VI (Andres & Langston, 2021). The latter interpretation is corroborated here, as explored further below.

The postzygapophyseal pedicles exhibit robust epipophyses, as typical of azhdarchid cervicals (e.g. Averianov, 2010; Andres & Langston, 2021). The long axis of each epipophysis

curves medially, similar to the sixth cervical of *Quetzalcoatlus lawsoni* (Andres & Langston, 2021). Still, as seen from the posterior view, the outer edge of each epipophysis is strongly curved medially, much more markedly than in *Quetzalcoatlus lawsoni* or any other azhdarchid (Fig. 4). Furthermore, the anterodorsal surface of each epipophysis is distinctively keeled, similar to the condition seen in the atlantoaxis (suggesting this feature may have been general for the cervical series in this taxon). This differs from the usual condition seen in other azhdarchids wherein the dorsal epipophyseal surface is blunt, as seen in *Quetzalcoatlus lawsoni* (all mesocervicals; Andres & Langston, 2021), *Cryodrakon boreas* (Hone *et al.*, 2019), the Bissekty azhdarchid material referred to *Azhdarcho lancicollis* (all mesocervicals; Averianov, 2010), *Quetzalcoatlus* cf. *northropi* (Andres & Langston, 2021), *Albadraco tharmisensis* (Solomon *et al.*, 2019), and the Bakony azhdarchid (Ősi *et al.*, 2005). Similarly, the *Nipponopterus mifunensis* also exhibits epipophyses with a sharp dorsal surface (Ikegami *et al.*, 2000; Zhou *et al.*, 2024). However, this condition is slightly distinct in this form. In *Nipponopterus mifunensis*, CVI bears a pair of elevated, distinct keels that extend throughout the entire dorsal surface of the postzygapophyseal peduncles, including the epipophyses (Zhou *et al.*, 2024).

The dorsal surface exhibits dorsally reflected transverse ridges (Fig. 4A, D), similar to MPC−Nd 100/302b as well as *Quetzalcoatlus lawsoni*, *Arambourgiania philadelphiae*, and *Nipponopterus mifunensis* (Andres & Langston, 2021; Zhou *et al.*, 2024). The interpostzygapophyseal lamina is sinusoidal (in dorsal view), with a convex mid-region, similar to cervicals VI and VII of *Quetzalcoatlus lawsoni* but unlike cervical V in which this lamina is concave (Andres & Langston, 2021). The posterior neural opening is higher than wide and is piriform in shape, with an acuminated apex. The neural canal is bordered by a small pair of adjacent pneumatic foramina, which are aligned with the center of the neural canal opening. There is no individualized accessory pneumatic foramen dorsal to the neural canal.

The condyle is ovoid in shape, with a prominently convex dorsal margin in posterior view, similar to cervical VI (and unlike the cordate shape seen in other mesocervicals) of *Quetzalcoatlus lawsoni* (Andres & Langston, 2021). A pair of postexapophyses are present lateroventrally to the condyle, as typical of ornithocheiroids as well as of ctenochasmatids (Andres & Ji, 2008; Andres, 2021). Similar to cervical III, the postexapophyses of cervical VI are relatively reduced in anteroposterior length, barely extending the posterior limits of the

condyle when seen in dorsal view (Fig. 4A, D). This contrasts with the mesocervicals of other azhdarchids, especially considering that in the complete cervical series of *Quetzalcoatlus lawsoni* the postexapophyses of CVI are the longest ones (Andres & Langston, 2021). On the posterior surface of the centrum, a well-developed horizontal lamina connects the two postexapophyses, again similar to cervical III (Fig. 4C, H). This feature, hereby termed an interpostexapophyseal lamina, is unique to *Gobiazhdarcho tsogtbaatari*, being absent in any other known azhdarchid cervicals. The ventral surface of the postexapophyses bears a set of five ventral parasagittal ridges, organized as follows. Each postexapophysis exhibits two ventral parasagittal ridges, and a single ventral parasagittal ridge is further present between the two postexapophyses (Fig. 4B, E). This feature is also unique to *Gobiazhdarcho tsogtbaatari*.

We corroborate here the interpretation of Andres & Langston (2021), identifying element MPC−Nd 100/302c as a cervical VI. Most notably, the posterior condyle is ovoid in shape when seen in posterior view, with a notoriously convex dorsal margin. If compared to the cervical series of *Quetzalcoatlus lawsoni*, this is most similar to cervical VI, and distinct from the rather cordate shape seen in cervicals IV, V, and VII (Andres & Langston, 2021). Furthermore, we consider MPC−Nd 100/302c unlikely to represent a cervical IV due to the lack of a posterior deflection of the centrum (Andres & Langston, 2021).

Ontogenetic assessment. Inferring ontogenetic stages in pterosaurs is a controversial task subject (Bennett, 1995; Kellner, 2015; Dalla Vecchia, 2018). Based on current evidence, it is clear that, during pterosaur ontogeny, the fusion between neural arches and centra is asynchronous throughout the vertebral column, and it is also clear that this occurs early in ontogeny concerning cervical vertebrae (e.g. Eck *et al.*, 2011; Shen *et al.*, 2020). In contrast, fusion between atlas and axis (forming the atlantoaxis complex) seems restricted to individuals that are close to osteological maturity (e.g. Kellner, 2015). Therefore, full atlantoaxis fusion in MPC−Nd 100/302 indicates that it is close to osteological maturity. Furthermore, specimen MPC−Nd 100/302 also exhibits a fairly smooth and dense bone surface, which is typical of adult pterosaur bones (e.g. Bennett, 1995), including cervicals (Vremir *et al.*, 2015; Longrich *et al.*, 2018; Hone *et al.*, 2019; Smith *et al.*, 2023). This is unlike the “grained texture” found in young pterosaur bones (e.g. Bennett, 1995), including cervicals (Hone *et al.*, 2019; Solomon *et al.*, 2019). On the other hand, the third cervical of MPC−Nd 100/302 lacks fused ribs. This suggests

that MPC−Nd 100/302 was close to, but had not yet reached, full osteological maturity, and may be regarded as a late subadult.

Hatzegopterygia new clade name (Table 1)

Tsogtopteryx mongoliensis gen. et sp. nov.

Holotype. MPC−Nd 100/303, the Bayshin Tsav azhdarchid (Watabe *et al.*, 2009). The specimen comprises an almost complete cervical VI (Fig. 5).

Etymology. The generic epithet is a combination of the words *Tsogt* (as in Tsogtbaatar; Mongolian: *mighty hero*) and *pteryx* (Ancient Greek: *wing*). The specific epithet refers to the provenance of the type specimen.

Type locality and horizon. Northwestern part of the Bayshin Tsav locality, Southern Gobi Aimag (Watabe *et al.*, 2009). Upper Bayanshiree Formation, Turonian–Santonian (see Averianov & Sues, 2012).

Diagnostic apomorphies. CVI prezygapophyseal pedicle bearing a ventral keel; centrum bearing a pair of longitudinal ventrolateral ridges.

Description and comparisons. MPC−Nd 100/303 is an elongated mesocervical vertebra. It is almost completely preserved, except for the posterior region. The element is broken posteriorly at about the level of the base of the postzygapophyseal pedicles, so that the postzygapophyses, posterior vestibule, condyle, and postexapophyses are missing. The neural spine is bifid, divided into anterior and posterior processes. The anterior process is conspicuously larger than the posterior one, as in *Albadraco tharmisensis* (Solomon *et al.*, 2019), the Pui azhdarchid (Vremir *et al.*, 2015), *Cryodrakon boreas* (Hone *et al.*, 2019), and, to a lesser extent, cf. *Hatzegopteryx thambema* (Vremir, 2010). In dorsal view, the lateral margins are gently curved, but the vertebral shaft does not exhibit a strong constriction. The transverse ridges are positioned laterally (Fig. 5), as in *Azhdarcho lancicollis* (Averianov, 2010), *Cryodrakon boreas* (Hone *et al.*, 2019), and *Phosphatodraco mauritanicus* (Longrich *et al*., 2018), and unlike the dorsally reflected condition seen in the Burkhant azhdarchid (see above), *Nipponopterus mifunensis* (Zhou *et al.*, 2024), *Quetzalcoatlus lawsoni*, and *Arambourgiania philadelphiae* (Andres & Langston, 2021). The

centrum exhibits a pair of ventrolateral longitudinal ridges that extend, on each side, from the base of the prezygapophyseal pedicle to the base of the postzygapophyseal pedicle (Fig. 5E–J). This feature is unique to the Bayshin Tsav and absent in any other known azhdarchid specimen.

The anterior neural canal opening is piriform in shape (Fig. 5A, B), with an acuminated dorsal apex. It is bordered by a pair of adjacent foramina, with are level with the ventral half of the neural canal opening. The prezygapophyseal articular facets are piriform in shape, with posteriorly acuminated margins. The prezygapophyseal pedicle ventral surface lacks the large tubercle present in MPC−Nd 100/302b, and instead exhibits an elongated, sharp keel (Fig. 5E, F). The vestigial cervical rib is entirely fused to the vertebrae, enclosing a transverse foramen (Fig. 5A, B).

MPC−Nd 100/303 has been tentatively interpreted as a cervical IV by Averianov (2014), what was later followed by Andres & Langston (2021). However, as noted by Andres & Langston (2021), azhdarchid fourth cervicals tend to exhibit a posteriorly deflected centrum, a feature that is absent in MPC−Nd 100/303. The discrete lateral constriction and presence of a large notch in the interprezygapophyseal ridge, as found in the sixth cervicals of *Quetzalcoatlus lawsoni* and *Wellnhopterus brevirostris* (Andres & Langston, 2021), lead us to reinterpret MPC−Nd 100/303 as a cervical VI.

Ontogenetic assessment. Specimen MPC−Nd 100/303 exhibits a fairly smooth, dense bone surface texture, similar to MPC-Nd 100/302 (see above) and other azhdarchid specimens regarded as osteologically mature, such as the Pui azhdarchid (Vremir *et al.*, 2015) and *Phosphatodraco mauritanicus* FSAC-OB 12. The bone surface does not exhibit, anywhere, the "grained texture" that is typical of young pterosaur specimens (Bennett, 1995), which can be seen in the cervical vertebrae of the holotypes of *Cryodrakon boreas* (Hone *et al.*, 2019) and *Albadraco tharmisensis* (Solomon *et al.*, 2019). In addition, the specimen exhibits (vestigial) cervical ribs fully fused to the vertebra (enclosing the transverse foramen), what is also characteristic of osteologically mature specimens (Longrich *et al.*, 2018; Andres & Langston, 2021). Therefore, MPC−Nd 100/303 can be regarded as an osteologically mature individual, despite its small size.

Phylogenetic analysis

Our phylogenetic analysis produced 27 most parsimonious trees, with 2177 steps, ensemble consistency index of 0.356 and ensemble retention index of 0.788 (Fig. 6). Similar to previous analyses (Andres, 2021), azhdarchids are characterized by three synapomorphies: character 320(2), mesocervical vertebrae neural spines vestigial (bifid; composed of anterior and posterior neural processes, connected by a neural ridge); 346(3), mid-cervical vertebrae extremely elongated (maximum length/width ratio over 5); and 481(3), wing digit phalanges 2 and 3 bearing a ventral keel (ambiguous; unknown in alanqids). Of note, the bifid vestigial neural spines of azhdarchids set them apart from non-azhdarchid azhdarchiforms (see Andres, 2021), which exhibit low/reduced but not bifid/vestigial neural spines, as seen in *Montanazhdarcho minor* (see Andres, 2021) and alanqids (see Williams *et al.*, 2020).

The earliest diverging azhdarchid branch is represented by Phosphatodraconia (Table 1; Fig. 6), supported by character 326(1), absence of adjacent foramina on the mesocervical vertebrae (unknown in *Wellnhopterus*); and 335(1), centrum lateral margins subparallel (ambiguous; unknown in *Aralazhdarcho*). The remaining azhdarchids are joined in a clade, to the exclusion of phosphatodraconians, on the basis of: character 14(0), nasoantorbital fenestra under half of skull length; character 206(1), downcurved mandibular rami; and character 347(1), CVI longer than CIV. The newly defined Quetzalcoatlida is supported by four synapomorphies: character 39(1), jaw tomial edges reduced/rounded; character 184 (0), ventralized posterior palate, forming a suspensorium; character 325(1), mesocervical neural canal opening higher-than-wide (in mature forms; presumably confluent neural canal opening and accessory foramen); and character 521(0), femur shaft strongly bowed (ambiguous; unknown in *Azhdarcho*). See the Discussion for further comments.

Hatzegopterygia is supported by character 321(1), anterior spinous process larger than the posterior one. This character supports placement of *Tsogtopteryx mongoliensis* within the clade. The clade containing the remaining hatzegopterygians, to the exclusion of *Tsogtopteryx mongoliensis*, is supported by character 346(2), mesocervical vertebrae only moderately elongated (length/width ratio under 5). This last feature can be seen in cf. *Hatzegopteryx thambema* (Vremir, 2010; Witton & Naish, 2017), the Pui azhdarchid (Vremir *et al.*, 2015), *Albadraco tharmisensis* (Solomon *et al.*, 2019), and *Cryodrakon boreas* (Hone *et al.*, 2019).

Quetzalcoatlini is supported by the following two synapomorphies: character 333(1), mesocervical vertebrae transverse ridges dorsally reflected; and 341(1), mesocervical vertebrae with lateral excavation between postzygapophysis and postexapophysis. These two characters support placement of *Gobiazhdarcho tsogtbaatari* within this group. This species lies as the sister-taxon of *Nipponopterus mifunensis* (as previously recovered by Zhou *et al.*, 2024), with which it shares character 332(1), dorsally keeled epipophyses; and 340(1), reduced postexapophyses. The clade containing all remaining quetzalcoatlinins is supported by character 342(1), mesocervical vertebrae with a well-developed ventral fossa between the postexapophyses (delineated by an anterior rim).

Discussion

The Bayanshiree Formation azhdarchids

According to the present interpretation, the holotypes of *Gobiazhdarcho tsogtbaatari* and *Tsogtopteryx mongoliensis* can be directly compared on the basis of the morphology of cervical VI, which is the only element with preserved overlap between the two specimens. Most importantly, *Tsogtopteryx mongoliensis* exhibits, autapomorphically, a pair of ventrolateral ridges running long the centrum of CVI, which are absent in *Gobiazhdarcho tsogtbaatari*. Furthermore, *Gobiazhdarcho tsogtbaatari* exhibits dorsally reflected transverse ridges and a well-developed posterior lateral fossa (between the postzygapophyses and postexapophyses), both of which are shared with other quetzalcoatlinins but are absent in *Tsogtopteryx mongoliensis*.

It is important to note that, according to the present results, the Burkhant and Bayshin Tsav azhdarchids nest within distinct azhdarchid lineages. *Gobiazhdarcho tsogtbaatari* can be clearly assigned to the Quetzalcoatlini, particularly due to the presence of dorsally reflected transverse ridges and a well-developed posterior lateral fossa (as seen in *Quetzalcoatlus lawsoni* and *Arambourgiania philadelphiae*). These features are absent in *Tsogtopteryx mongoliensis*. In contrast, *Tsogtopteryx mongoliensis* exhibits affinities to Hatzegopterygia instead (particularly due to the anterior spinous process being larger than the posterior one), reinforcing the distinctiveness between the two taxa. At a late-Turonian–Santonian age, *Tsogtopteryx*

mongoliensis partially fills a temporal gap within Hatzegopterygia, as the hatzegopterygian lineage was previously restricted to the Maastrichtian (Pêgas *et al.*, 2021; Andres, 2021), even though quetzalcoatlinins extend from the Turonian–Coniacian to the Maastrichtian (Zhou *et al.*, 2024).

Regarding body size, estimates for fragmentary fossil specimens are always filled with uncertainty, especially when it comes to groups with a great diversity of skeletal proportions such as azhdarchids (Cai & Wei, 1994; Naish & Witton, 2017; Andres & Langston, 2021). Nonetheless, based on anterior and posterior widths at the zygapophyses as compared to more complete skeletons (such as those of *Q. lawsoni*, *C. boreas*, *M. maggi*, and *Z. linhaiensis*), we herein estimate *Gobiazhdarcho tsogtbaatari* as a medium pterosaur (3.0–3.5 m), and *Tsogtopteryx mongoliensis* as a small one (~1.6–1.9 m wingspan) (see Supplemental File 3 for further details). It is interesting to note that *Tsogtopteryx mongoliensis* represents one of the smallest known azhdarchid species so far, only behind the ~1.6 meter-wingspan Hornby ?azhdarchid, from the Campanian of Canada (Martin-Silverstone *et al.*, 2016).

It is interesting to note that the Bayanshiree Formation reinforces the reoccurring (though not universal) pattern of multiple, variably-sized azhdarchid species being present in a same deposit (Fig. 7). This pattern has been explored in detail before, based on the co-occurrence of the medium (3 m wingspan) *Wellnhopterus brevirostris*, the large (5 m) *Quetzalcoatlus lawsoni*, and the giant (10 m) *Quetzalcoatlus northropi* in the Javelina Fm. (Andres & Langston, 2021). Similarly, the medium (3 m) Pui azhdarchid, the large (>5 m) *Albadraco tharmisensis*, and the giant (10 m) *Hatzegopteryx thambema* can all be found in the late Maastrichtian of Haţeg Island (Vremir *et al.*, 2015; Solomon *et al.*, 2019); while the medium (3 m) *Eurazhdarcho langendorfensis* and the giant (~10 m) cf. *Hatzegopteryx* sp. (LPB R2347) both stem from the early Maastrichtian of Haţeg Island (Vremir *et al.*, 2013; 2018). In the late Maastrichtian of the Ouled Abdoun Basin, at least three azhdarchid species can also be found: the medium (~3 m) aff. *Quetzalcoatlus* sp., the large (4–5 m) *Phosphatodraco mauritanicus*, and the giant (~9 m) cf. *Arambourgiania philadelphiae* (Longrich *et al.*, 2018).

Comments on azhdarchid intrarelationships

According to the present phylogenetic hypothesis, the Azhdarchidae can be subdivided into four main lineages: Phosphatodraconia, a *Zhejiangopterus*-clade, *Azhdarcho*, and Quetzalcoatlida (Fig. 6). A clade (*i.e.* Quetzalcoatlida) that includes only *Quetzalcoatlus*, *Arambourgiania*, *Hatzegopteryx*, and their respective most closely related forms, to the exclusion of *Azhdarcho lancicollis*, *Zhejiangopterus linhaiensis*, and phosphatodraconians, seems well established (Andres *et al.*, 2014; Andres, 2021; Pêgas *et al.*, 2021; 2023; Zhou *et al.*, 2024). Exactly what further taxa belong within this subclade, or not, remain slightly contentious (e.g. Longrich *et al.*, 2018; Andres, 2021; Pêgas, 2024). Nevertheless, the Quetzalcoatlida as herein proposed is still comparatively stable across distinct phylogenetic proposals; applying to roughly similar clades (regarding composition and diagnosis) under both the present reference phylogeny and alternative ones (e.g. Andres, 2021). This is in contrast with the branch-based clade Quetzalcoatlinae *sensu* Andres (2021), which is comparatively much more unstable in composition (see Andres, 2021; Zhou *et al.*, 2024). The Quetzalcoatlida can be characterized by four synapomorphies: jaw tomial edges reduced; ventralized pterygoid, forming a suspensorium; presence of a higher-than-wide neural canal opening (in mature forms); and femur shaft strongly bowed (see Phylogenetic Analysis).

The typical higher-than-wide neural canal opening of quetzalcoatlidans is postulated to derive from a confluence between the neural canal opening and the accessory foramen (see Andres & Langston, 2021; Zhou *et al.*, 2024). This is evidenced from the clithridiate ("keyhole-shaped") neural canals found in *Arambourgiania philadelphiae* (Martill *et al.*, 1998), cf. *Hatzegopteryx thambema* (see Naish & Witton, 2017), the Pui azhdarchid (Vremir *et al.*, 2015), *Quetzalcoatlus lawsoni* (see Andres & Langston, 2021), *Gobiazhdarcho tsogtbaatari* (present work), and *Nipponopterus mifunensis* (Zhou *et al.*, 2024). Non-quetzalcoatlidan azhdarchids exhibit circular neural canal openings, whether an accessory foramen is present, as in *Azhdarcho lancicollis* (Nessov, 1984; Averianov, 2010) and *Phosphatodraco mauritanicus* (Longrich *et al.*, 2018); or absent (entirely lost), as in the Bakony azhdarchid (Ősi *et al.*, 2005) and *Mistralazhdarcho maggi* (Vullo *et al.*, 2018).

Within the *Quetzalcoatlus lawsoni* hypodigm, while all neural canals are higher-than-wide, some are clearly clithridiate while others exhibit attenuated/acuminated dorsal margins and less accentuated waists (Andres & Langston, 2021). This also contrasts with the typical

subcircular condition, and similar shapes can be found in *Tsogtopteryx mongoliensis* (present work) and *Albadraco tharmisensis* (Solomon *et al.*, 2019). Such variation seems related to serial variation within the cervical series (see Averianov, 2010; Andres & Langston, 2021).

When present, the confluence between the accessory foramen and the neural canal opening seems to be an ontogenetic feature. As noted by Nessov (1984), some Bissekty azhdarchid specimens seem to exhibit varying levels of incipiently confluent accessory foramina and neural canal openings (suggesting the presence of quetzalcoatlidans in the Bissekty azhdarchid assemblage). In *Cryodrakon boreas*, some indication that such incipient confluence could be ontogenetic in nature can also be found. In the holotype of *Cryodrakon boreas*, which is a juvenile specimen (Hone *et al.*, 2019), the preserved mid-cervical (65 mm between prezygapophyses) exhibits distinct accessory foramen and neural canal openings, separated by a well-developed bony bar of regular shape. By contrast, in the larger specimens TMP 1993.40.11 (mid-cervical 82 mm between prezygapophyses) and TMP 1989.36.254 (mid-cervical 97 mm between prezygapophyses), the accessory foramen and neural canal openings are separated by an incipient (extremely thin) bony bar of irregular shape (see Hone *et al.*, 2019). Interestingly, in these specimens, the accessory foramen is larger than the neural canal opening, unlike in the holotype wherein the reverse is true. This pattern suggests that, with ontogeny, the accessory foramen expands while the bony bar that separates it from the neural canal opening is reabsorbed (hence its thin, irregular configuration in the larger specimens), ultimately leading to a possible confluence between the accessory foramen and the neural canal opening (note that none of these specimens is fully mature, as indicated by the lack of cervical rib fusion; see Hone *et al.*, 2019). Therefore, we suggest caution regarding the assessment of the presence, or absence, of this feature in azhdarchid taxa. We suggest it can only be confidently assessed when osteologically mature specimens are available, and reiterate that future studies with more complete ontogenetic series will be needed in order to confirm this.

As herein proposed, the Quetzalcoatlida comprise two main lineages: the Hatzegopterygia and the Quetzalcoatlini. A clade comprising the Transylvanian azhdarchids *Hatzegopteryx thambema* and *Albadraco tharmisensis* had already been recovered by Pêgas *et al.* (2021; 2023); to this clade, Hatzegopterygia, we now assign also *Cryodrakon boreas*, the Pui azhdarchid, and the new species *Tsogtopteryx mongoliensis*. This new phylogenetic structure

extends the stratigraphic range of this lineage, previously restricted to the Maastrichtian, back to the Turonian–Santonian. According to the present phylogeny, hatzegopterygians are united by a distinctive feature on the bifid neural spine of the mesocervical series: the anterior spinous process is larger (longer and wider) than the posterior one, unlike other azhdarchids. This feature does not seem to be influenced by serial variation, as demonstrated by the cervical series of *Quetzalcoatlus lawsoni* and *Wellnhopterus brevirostris* (Andres & Langston, 2021).

It is interesting to note that, to the exclusion of the basal form *Tsogtopteryx mongoliensis*, the remaining hatzegopterygians exhibit relatively robust mesocervicals, starkly departing from the typical slender-necked bauplan of other azhdarchids. The existence of a "robust-necked" azhdarchid bauplan was first indicated by the discoveries of cf. *Hatzegopteryx* EME 315 (Vremir, 2010) and the Pui azhdarchid (Vremir *et al.*, 2015), and later discussed in detail by Naish & Witton (2017). These discoveries indicate that these forms developed secondarily shorter necks relative to other azhdarchids, what implicates in a distinct neck biomechanical performance and, in all likelihood, a distinct ecology (Naish & Witton, 2017). *Hatzegopteryx*, the Pui azhdarchid, and *Albadraco* had already been recognized as "robust-necked" azhdarchids before (Vremir *et al.*, 2015; Naish & Witton, 2017; Solomon *et al.*, 2019), and *Cryodrakon boreas* seems to represent at least an "intermediate morphology" regarding robustness (see Hone *et al.*, 2019).

In turn, Quetzalcoatlini comprises all quetzalcoatlidans closer to *Quetzalcoatlus northropi* than to *Hatzegopteryx thambema* (Table 1). At the base of this clade lie *Gobiazhdarcho tsogtbaatari* and *Nipponopterus mifunensis*, which share with other quetzalcoatlinins the following two features: dorsally reflected transverse ridges, and a well-developed lateral fossa between the potzygapophyses and postexapophyses (Zhou *et al.*, 2024). The dorsally reflected ridges can be seen in remains of *Arambourgiania philadelphiae* (Frey & Martill, 1996), *Quetzalcoatlus lawsoni* (Andres & Langston, 2021), and aff. *Quetzalcoatlus* sp. (Longrich *et al.*, 2018), aside from *Gobiazhdarcho tsogtbaatari* and *Nipponopterus mifunensis* (Zhou *et al.*, 2024). Regarding the lateral fossa between the potzygapophyses and postexapophyses, this feature is bordered ventrally by a sharp flange that protrudes from the lateral surface of the postexapophyseal peduncle. This latter feature can be particularly well-seen in remains of *Quetzalcoatlus lawsoni* and cf. *Quetzalcoatlus northropi* (Andres & Langston, 2021), aside from

Gobiazhdarcho tsogtbaatari. This feature is also present in *Wellnhopterus brevirostris* (see Andres & Langston, 2021), although this is recovered here as a homoplasy. Interestingly, this lateral fossa bears a pneumatic opening in remains of cf. *Arambourgiania philadelphiae* (Martill & Moser, 2018). To the exception of *Gobiazhdarcho tsogtbaatari*, the remaining quetzalcoatlinins further share a well-defined ventral fossa between the postexapophyses (delineated by an anterior rim), as seen in remains of cf. *Quetzalcoatlus northropi*, *Quetzalcoatlus lawsoni* (Andres & Langston, 2021), aff. *Quetzalcoatlus* sp. (Longrich *et al.*, 2018), and *Arambourgiania philadelphiae* (Martill & Moser, 2018).

Conclusions

The present anatomical reassessment of the Bayanshiree Fm. azhdarchids reveals several features that distinguish the Burkhant and Bayshin Tsav specimens from each other, as well as from other azhdarchids. These specimens are accordingly recognized here as new species, with the Burkhant azhdarchid representing a new quetzalcoatlinin, *Gobiazhdarcho tsogtbaatari*, and the Bayshin Tsav azhdarchid representing a new hatzegopterygian, *Tsogtopteryx mongoliensis*. These forms reiterate the general pattern of a single deposit yielding multiple azhdarchid species of distinct body sizes, with *Tsogtopteryx mongoliensis* being notoriously small for an azhdarchid (with a wingspan of ~1.6–1.9 m) whereas *Gobiazhdarcho tsogtbaatari* represents a medium (3.0–3.5 m) pterosaur. Apart from enhancing our understanding of the diversity of the Bayanshiree Fm., the recognition of these two new species also fills in important temporal gaps in the evolutionary history of azhdarchids.

Acknowledgements

We are deeply grateful to Khishigjav Tsogtbaatar (MPC) for encouraging the development of the present research. We also acknowledge Mr. Ken Hayashibara (president of the Hayashibara Company Limited, Okayama, Japan) and all participants of the *Hayashibara Museum of Natural Sciences-Mongolian Paleontological Center Joint Paleontological Expeditions* for their

722 contributions to Mongolian paleontology. We further thank the Willi Hennig Society for making
723 TNT freely available, and Zhao Chuang for kindly providing his superb artwork.

724

725 **References**

726 Agnolín, F., Rozadilla, S., Juárez-Valieri, R., & Meso, J. (2023). Oldest azhdarchid (Pterosauria)
727 record from South America. *Revista del Museo Argentino de Ciencias Naturales nueva*
728 *serie*, *25*(2), 309-314.

729 Aires, A. S., Kellner, A. W., Müller, R. T., Da Silva, L. R., Pacheco, C. P., & Dias-Da-Silva, S.
730 (2014). New postcranial elements of the Thalassodrominae (Pterodactyloidea,
731 Tapejaridae) from the Romualdo Formation (Aptian–Albian), Santana Group, Araripe
732 Basin, Brazil. *Palaeontology*, *57*(2), 343-355.

733 Andres, B. (2021). Phylogenetic systematics of Quetzalcoatlus Lawson 1975 (Pterodactyloidea:
734 Azhdarchoidea). *Journal of Vertebrate Paleontology*, *41*(sup1), 203-217.

735 Andres, B., & Langston Jr, W. (2021). Morphology and taxonomy of Quetzalcoatlus Lawson
736 1975 (Pterodactyloidea: Azhdarchoidea). *Journal of Vertebrate Paleontology*, *41*(sup1),
737 46-202.

738 Andres, B., and K. Padian. 2020a. Pterosauria†; pp. 1201–1204 in K. de Queiroz, P. D. Cantino,
739 and J. A. Gauthier (eds.), Phylonyms. A Companion to the PhyloCode. CRC Press, Boca
740 Raton, FL.

741 Andres, B., and K. Padian. 2020b. Pterodactyloidea†; pp. 1205–1208 in K. de Queiroz, P. D.
742 Cantino, and J. A. Gauthier (eds.), Phylonyms. A Companion to the PhyloCode. CRC
743 Press, Boca Raton, FL.

744 Andres, B., Clark, J., & Xu, X. (2014). The earliest pterodactyloid and the origin of the
745 group. *Current Biology*, *24*(9), 1011-1016.

746 Andrews, C. (1932). *The new conquest of central Asia a narrative of the explorations of the*
747 *Central Asiatic expeditions in Mongolia and China, 1921-1930*. Рипол Классик.

748 Averianov, A. O. (2010). The osteology of Azhdarcho lancicollis Nessov, 1984 (Pterosauria,
749 Azhdarchidae) from the late Cretaceous of Uzbekistan. *Proceedings of the Zoological*
750 *Institute RAS*, *314*(3), 264-317.

751 Averianov, A. O. (2014). Review of taxonomy, geographic distribution, and paleoenvironments
752 of Azhdarchidae (Pterosauria). *ZooKeys*, (432), 1.

753 Averianov, A., & Sues, H. D. (2012). Correlation of Late Cretaceous continental vertebrate
754 assemblages in Middle and Central Asia. *Journal of Stratigraphy*.

755 Bakhurina, N. N. 1982. [A pterodactyl from the Lower Cretaceous of Mongolia].
756 Palaeontologicheskii Zhurnal 4, 104–8 (in Russian).

757 Bakhurina, N. N. 1986. Flying reptile. Priroda 7, 27–36 (in Russian).

758 Bakhurina, N. N., & Unwin, D. M. (1995). A survey of pterosaurs from the Jurassic and
759 Cretaceous of the former Soviet Union and Mongolia.

760 Barsbold, R., Kobayashi, Y., & Kubota, K. (2007, September). New discovery of dinosaur
761 fossils from the Upper Cretaceous Bayanshiree Formation of Mongolia. In *Journal of*
762 *Vertebrate Paleontology* (Vol. 27, No. 3, pp. 44A-44A).

763 Bennett, S. C. (1993). The ontogeny of *Pteranodon* and other pterosaurs. *Paleobiology*, *19*(1),
764 92-106.

765 Bennett, S. C. (1994). Taxonomy and systematics of the late Cretaceous pterosaur *Pteranodon*
766 (Pterosauria, Pterodactyloidea). *Occasional Papers of the Natural History Museum of the*
767 *University of Kansas*, *169*, 1-70.

768 Benton, M. J., Shishkin, M. A., Unwin, D. M., & Kurochkin, E. N. (Eds.). (2000). *The age of*
769 *dinosaurs in Russia and Mongolia*. Cambridge University Press.

770 Buchmann, R., & Rodrigues, T. (2019). The evolution of pneumatic foramina in pterosaur
771 vertebrae. *Anais Da Academia Brasileira De Ciencias*, *91*, e20180782.

772 Buffetaut, E., Grigorescu, D., & Csiki, Z. (2002). A new giant pterosaur with a robust skull from
773 the latest Cretaceous of Romania. *Naturwissenschaften*, *89*, 180-184.

774 Cai, Z. and Wei, F. 1994. On a new pterosaur (*Zhejiangopterus linhaiensis* gen. et sp. nov.) from
775 Upper Cretaceous in Linhai, Zhejiang, China. *Vertebrata Palasiatica* 32: 181–194

776 Cerqueira, G. M., Santos, M. A., Marks, M. F., Sayão, J. M., & Pinheiro, F. L. (2021). A new
777 azhdarchoid pterosaur from the Lower Cretaceous of Brazil and the paleobiogeography of
778 the Tapejaridae. *Acta Palaeontologica Polonica*, *66*(3), 555-570.

779 Colbert, E. H. (2000). Asiatic dinosaur rush. In: Benton, M. J., Shishkin, M. A., Unwin, D. M., &
780 Kurochkin, E. N. (Eds.), The Age of Dinosaurs in Russia and Mongolia, Cambridge
781 University Press, pp. 211-234.

782 Dalla Vecchia, F. M. (2009). Anatomy and systematics of the pterosaur *Carniadactylus* gen. n.
783 *rosenfeldi* (Dalla Vecchia, 1995). *Rivista Italiana di Paleontologia e stratigrafia*, *115*(2),
784 159-186.

785 Dalla Vecchia, F. M. (2018). Comments on Triassic pterosaurs with a commentary on the"
786 ontogenetic stages" of Kellner (2015) and the validity of Bergamodactylus wildi. *Rivista*
787 *Italiana di Paleontologia e Stratigrafia*, *124*(2).

788 Dalla Vecchia, F. M. (2019). *Seazzadactylus venieri* gen. et sp. nov., a new pterosaur (Diapsida:
789 Pterosauria) from the Upper Triassic (Norian) of northeastern Italy. *PeerJ*, *7*, e7363.

790 Danilov, I. G., Hirayama, R., Sukhanov, V. B., Suzuki, S., Watabe, M., & Vitek, N. S. (2014).
791 Cretaceous soft-shelled turtles (Trionychidae) of Mongolia: new diversity, records and a
792 revision. *Journal of Systematic Palaeontology*, *12*(7), 799-832.

793 de Queiroz, K., & Cantino, P. (2020). *International code of phylogenetic nomenclature*
794 *(PhyloCode)*. CRC Press.

795 de Queiroz, K., Cantino, P., & Gauthier, J. (2020). *Phylonyms: a Companion to the PhyloCode*.
796 CRC Press.

797 Eck, K., Elgin, R. A., & Frey, E. (2011). On the osteology of *Tapejara wellnhoferi* Kellner 1989
798 and the first occurrence of a multiple specimen assemblage from the Santana Formation,
799 Araripe Basin, NE-Brazil. *Swiss Journal of Palaeontology*, *130*(2), 277-296.

800 Frey, E., Martill, D.M., 1996. A reappraisal of *Arambourgiania* (Pterosauria, Pterodactyloidea),
801 one of the world's largest flying animals. Neues Jahrbuch für Geologie und Palaontologie,
802 Abhandlungen 199, 221–247.

803 Goloboff, P.A., Catalano, S.A., 2016. TNT version 1.5, including a full implementation of
804 phylogenetic morphometrics. Cladistics 32 (3), 221e238.

805 Hicks, J. F., Brinkman, D. L., Nichols, D. J., & Watabe, M. (1999). Paleomagnetic and
806 palynologic analyses of Albian to Santonian strata at Bayn Shireh, Burkhant, and Khuren
807 Dukh, eastern Gobi Desert, Mongolia. *Cretaceous Research*, *20*(6), 829-850.

808 Holgado, B., Pêgas, R. V., Canudo, J. I., Fortuny, J., Rodrigues, T., Company, J., & Kellner, A.
809 W. (2019). On a new crested pterodactyloid from the Early Cretaceous of the Iberian
810 Peninsula and the radiation of the clade Anhangueria. *Scientific Reports*, *9*(1), 4940.

811 Hone, D. W., Habib, M. B., & Therrien, F. (2019). *Cryodrakon boreas*, gen. et sp. nov., a Late
812 Cretaceous Canadian azhdarchid pterosaur. *Journal of Vertebrate Paleontology*, *39*(3),
813 e1649681.

814 Howse, S. C. B. (1986). On the cervical vertebrae of the Pterodactyloidea (Reptilia:
815 Archosauria). *Zoological Journal of the Linnean Society*, *88*(4), 307-328.

816 Ibrahim, N., Unwin, D. M., Martill, D. M., Baidder, L., & Zouhri, S. (2010). A new pterosaur
817 (Pterodactyloidea: Azhdarchidae) from the Upper Cretaceous of Morocco. *PLoS*
818 *One*, *5*(5), e10875.

819 Ikegami, N., Kellner, A. W. A., & Tomida, Y. (2000). The presence of an azhdarchid pterosaur
820 in the Cretaceous of Japan. *Paleontological Research*, *4*(3), 165-170.

821 Jagielska, N., & Brusatte, S. L. (2021). Pterosaurs. *Current Biology*, *31*(16), R984-R989.

822 Jerzykiewicz, T., & Russell, D. A. (1991). Late Mesozoic stratigraphy and vertebrates of the
823 Gobi Basin. *Cretaceous Research*, *12*(4), 345-377.

824 Kellner, A. W. A. (2003). Pterosaur phylogeny and comments on the evolutionary history of the
825 group. *Geological Society, London, Special Publications*, *217*(1), 105-137.

826 Kellner, A. W. A. (2004). New information on the Tapejaridae (Pterosauria, Pterodactyloidea)
827 and discussion of the relationships of this clade. *Ameghiniana*, *41*(4), 521-534.

828 Kellner, A. W. A. (2015). Comments on Triassic pterosaurs with discussion about ontogeny and
829 description of new taxa. Anais da Academia Brasileira de Ciências, 87, 669-689.

830 Kellner, A. W. A., Weinschütz, L. C., Holgado, B., Bantim, R. A., & Sayao, J. M. (2019). A new
831 toothless pterosaur (Pterodactyloidea) from Southern Brazil with insights into the
832 paleoecology of a Cretaceous desert. *Anais da Academia Brasileira de Ciências*, *91*.

833 Kielan-Jaworowska, Z. 1969. Hunting for Dinosaurs. 177 pp. MIT Press, Cambridge,
834 Massachusetts

835 Kobayashi, Y., & Barsbold, R. (2005). Reexamination of a primitive ornithomimosaur,
836 Garudimimus brevipes Barsbold, 1981 (Dinosauria: Theropoda), from the Late
837 Cretaceous of Mongolia. *Canadian Journal of Earth Sciences*, *42*(9), 1501-1521.

838 Kurochkin, E. N., & Barsbold, R. (2000). The Russian-Mongolian expeditions and research in
839 vertebrate paleontology. . In: Benton, M. J., Shishkin, M. A., Unwin, D. M., &
840 Kurochkin, E. N. (Eds.), The Age of Dinosaurs in Russia and Mongolia, Cambridge
841 University Press, pp. 235-255.

842 Kurumada, Y., Aoki, S., Aoki, K., Kato, D., Saneyoshi, M., Tsogtbaatar, K., ... & Ishigaki, S.
843 (2020). Calcite U–Pb age of the Cretaceous vertebrate-bearing Bayn Shire Formation in
844 the Eastern Gobi Desert of Mongolia: Usefulness of caliche for age determination. *Terra*
845 *Nova*, *32*(4), 246-252.

846 Lavas, J.R. 1993. Dragons from the Dunes: The search for dinosaurs in the Gobi Desert. 138 pp.
847 Academy Interprint Ltd., Auckland, 138 pp.

848 Lawson, D.A., 1975. Pterosaur from the Latest Cretaceous of West Texas. Discovery of the
849 largest flying creature. Science 187, 947e948

850 Longrich, N.R., Martill, D.M., Andres, B., Penny, D., 2018. Late Maastrichtian pterosaurs from
851 North Africa and mass extinction of Pterosauria at the CretaceousPaleogene boundary.
852 PLoS Biology 16 (3), e2001663

Lü, J., Azuma, Y., Dong, Z., Barsbold, R., Kobayashi, Y., Lee, Y.N. 2009. New material of dsungaripterid pterosaurs (Pterosauria, Pterodactyloidea) from western Mongolia and its palaeoecological implications. Geological Magazine 146 (5), 690e700.

Lü, J., Unwin, D. M., Jin, X., Liu, Y., & Ji, Q. (2009). Evidence for modular evolution in a long-tailed pterosaur with a pterodactyloid skull. *Proceedings of the Royal Society B: Biological Sciences*, *277*(1680), 383-389.

Martill, D. M., & Moser, M. (2018). Topotype specimens probably attributable to the giant azhdarchid pterosaur *Arambourgiania philadelphiae* (Arambourg 1959). *Geological Society, London, Special Publications*, *455*(1), 159-169.

Martin-Silverstone, E., Witton, M.P., Arbour, V.M., Currie, P.J., 2016. Small azhdarchoid pterosaur from the latest Cretaceous, the age of flying giants. Royal Society Open Science 3160333.

Martinson, G.G. 1975. [On the question of the principles of stratigraphy and correlation of the continental formations of Mongolia.] *Trudy Sovmesruoi SovetskoMongol'skoi Palcontologicheskoi Ekspeditsii* 13: 7-24

Martinson, G.G. 1982. [General problems of palaeolimnological studies in Mongolia.] pp. 5-17 in Martinson, G.G. (ed.), *Mesozoic Lake Basins of Mongolia.* Leningrad: Nauka

McPhee, J., Ibrahim, N., Kao, A., Unwin, D.M., Smith, R., & Martill, D.M. (2020). A new? chaoyangopterid (Pterosauria: Pterodactyloidea) from the Cretaceous Kem Kem beds of southern Morocco. *Cretaceous Research*, *110*, 104410.

Naish, D., & Witton, M. P. (2017). Neck biomechanics indicate that giant Transylvanian azhdarchid pterosaurs were short-necked arch predators. *PeerJ*, *5*, e2908.

Naish, D., Simpson, M., & Dyke, G. (2013). A new small-bodied azhdarchoid pterosaur from the Lower Cretaceous of England and its implications for pterosaur anatomy, diversity and phylogeny. *PloS one*, *8*(3), e58451.

Nessov, L.A., 1984. Upper Cretaceous pterosaurs and birds from Central Asia. Paleontologicheskii zhurnal 1, 47e57

880 Novacek, M. J. 1996. *Dinosaurs of the Flaming Cliffs*. New York: Doubleday, 369 pp.

881 Ortiz David, L.D., González Riga, B. J., & Kellner, A. W. 2022. *Thanatosdrakon amaru*, gen. et
882 sp. nov., a giant azhdarchid pterosaur from the Upper Cretaceous of
883 Argentina. *Cretaceous esearch*, *137*, 105228.

884 Ortiz-David, L.D., González Riga, B.J., Kellner, A.W.A., 2018. Discovery of the largest
885 pterosaur from South America. Cretaceous Research 83, 40e46.

886 Ősi, A., & Weishampel, D. B. (2005). First evidence of azhdarchid pterosaurs from the Late
887 Cretaceous of Hungary. *Acta Palaeontologica Polonica*, *50*(4), 777.

888 Owen, R. 1842. Report on British Fossil Reptiles, Part II: In Report of the Eleventh Meeting of
889 the British Association for the Advancement of Science, Vol. 1841, pp. 60–204. John
890 Murray, Plymouth.

891 Padian, K. 1986. A taxonomic note on two pterodactyloid families. Journal of Vertebrate
892 Paleontology 6:289.

893 Park, J. Y., Lee, Y. N., Currie, P. J., Kobayashi, Y., Koppelhus, E., Barsbold, R., ... & Kim, S. H.
894 (2020). Additional skulls of Talarurus plicatospineus (Dinosauria: Ankylosauridae) and
895 implications for paleobiogeography and paleoecology of armored dinosaurs. *Cretaceous*
896 *Research*, *108*, 104340.

897 Pêgas, R. V. (2024). A taxonomic note on the tapejarid pterosaurs from the Pterosaur Graveyard
898 site (Caiuá Group,? Early Cretaceous of Southern Brazil): evidence for the presence of
899 two species. *Historical Biology*, *2024*, 1-22.

900 Pêgas, R. V., Leal, M. E. C., & Kellner, A. W. A. (2016). A basal tapejarine (Pterosauria;
901 Pterodactyloidea; Tapejaridae) from the crato formation, Early Cretaceous of Brazil. *PloS*
902 *one*, *11*(9), e0162692.

903 Pêgas, R. V., Costa, F. R., & Kellner, A. W. (2018). New information on the osteology and a
904 taxonomic revision of the genus *Thalassodromeus* (Pterodactyloidea, Tapejaridae,
905 Thalassodrominae). *Journal of Vertebrate Paleontology*, *38*(2), e1443273.

Pêgas, R. V., Holgado, B., & Leal, M. E. C. (2019). On *Targaryendraco wiedenrothi* gen. nov.(Pterodactyloidea, Pteranodontoidea, Lanceodontia) and recognition of a new cosmopolitan lineage of Cretaceous toothed pterodactyloids. *Historical Biology*, *33*(8), 1266-1280.

Pêgas, R. V., Holgado, B., David, L. D. O., Baiano, M. A., & Costa, F. R. (2021). On the pterosaur *Aerotitan sudamericanus* (Neuquén Basin, Upper Cretaceous of Argentina), with comments on azhdarchoid phylogeny and jaw anatomy. *Cretaceous Research*, *129*, 104998.

Pêgas, R. V., Zhou, X., Jin, X., Wang, K., & Ma, W. (2023). A taxonomic revision of the *Sinopterus* complex (Pterosauria, Tapejaridae) from the Early Cretaceous Jehol Biota, with the new genus *Huaxiadraco*. *PeerJ*, *11*, e14829.

Perle, A. (1979). Segnosauridae—a new family of Theropoda from the Lower Cretaceous of Mongolia. *Trudy, Sovmestnaâ Sovetsko− Mongol'skaâ paleontologičeskaâ èkspediciâ*, *8*, 45-55.

Perle, A. (1981). A new segnosaurid from the Upper Cretaceous of Mongolia. Joint Soviet-Mongolian Paleontological Expedition. *Transactions*, *15*, 28-39.

Perle, A., Norell, M., & Clark, J. (1999). A new maniraptoran theropod, *Achillobator giganticus* (Dromaeosauridae), from the Upper Cretaceous of Burkhant, Mongolia. *Contrib. Dept. Geol. Natl Univ. Mongolia*, *101*, 1.

Plieninger, F. 1901. Beiträge zur Kenntnis der Flugsaurier. Palaeontographica 48:65–90.

Rougier, G. W., Davis, B. M., & Novacek, M. J. (2015). A deltatheroidan mammal from the Upper Cretaceous Baynshiree Formation, eastern Mongolia. *Cretaceous Research*, *52*, 167-177.

Rozhdestvenskii, A. K. 1960. *Cbasse aux Dinosaures dans le Desert de Gobi.* Paris: Librairie Artheme Favard.

Shen, C., Pêgas, R. V., Gao, C., Kundrát, M., Zhang, L., Wei, X., & Zhou, X. (2021). A new specimen of Sinopterus dongi (Pterosauria, Tapejaridae) from the Jiufotang Formation (Early Cretaceous, China). *PeerJ*, *9*, e12360.

934 Shuvalov, V. F. (2000). The Cretaceous stratigraphy and palaeobiogeography of Mongolia. *The*
935 *age of dinosaurs in Russia and Mongolia*.

936 Smith, R. E., Martill, D. M., & Zouhri, S. (2023). Distinctive azhdarchoid pterosaur jaws from
937 the mid-Cretaceous Cambridge Greensand of eastern England and the Kem Kem Group
938 of Morocco. *Proceedings of the Geologists' Association*.

939 Solomon, A. A., Codrea, V. A., Venczel, M., & Grellet-Tinner, G. (2020). A new species of
940 large-sized pterosaur from the Maastrichtian of Transylvania (Romania). *Cretaceous*
941 *Research*, *110*, 104316.

942 Suberbiola, X. P., Bardet, N., Jouve, S., Iarochène, M., Bouya, B., & Amaghzaz, M. (2003). A
943 new azhdarchid pterosaur from the Late Cretaceous phosphates of Morocco. *Geological*
944 *Society, London, Special Publications*, *217*(1), 79-90.

945 Tsogtbaatar, K., Weishampel, D. B., Evans, D. C., & Watabe, M. (2019). A new hadrosauroid
946 (Dinosauria: Ornithopoda) from the Late Cretaceous Baynshire Formation of the Gobi
947 Desert (Mongolia). *PLoS One*, *14*(4), e0208480.

948 Tsuihiji, T., Andres, B., O'connor, P. M., Watabe, M., Tsogtbaatar, K., & Mainbayar, B. (2017).
949 Gigantic pterosaurian remains from the Upper Cretaceous of Mongolia. *Journal of*
950 *Vertebrate Paleontology*, *37*(5), e1361431.

951 Turner, A. H. (2015). A review of Shamosuchus and Paralligator (Crocodyliformes, Neosuchia)
952 from the Cretaceous of Asia. *PLoS One*, *10*(2), e0118116.

953 Unwin, D. M. (1995). Preliminary results of a phylogenetic analysis of the Pterosauria (Diapsida:
954 Archosavria). In *Sixth symposium on mesozoic terrestrial ecosystems and biota* (pp. 69-
955 72).

956 Unwin, D. M. (2003). On the phylogeny and evolutionary history of pterosaurs. *Geological*
957 *Society, London, Special Publications*, *217*(1), 139-190.

958 Vidovic, S. U., & Martill, D. M. (2018). The taxonomy and phylogeny of *Diopecephalus kochi*
959 (Wagner, 1837) and *'Germanodactylus rhamphastinus'*(Wagner, 1851). *Geological*
960 *Society, London, Special Publications*, *455*(1), 125-147.

961 Vila Nova, B. C., Sayão, J. M., Langer, M. C., & Kellner, A. W. A. (2014). Comments on the
962 cervical vertebrae of the Tapejaridae (Pterosauria, Pterodactyloidea) with description of
963 new specimens. *Historical Biology*, *27*(6), 771-781.

964 Vremir, M. (2010). New faunal elements from the late Cretaceous (Maastrichtian) continental
965 deposits of Sebes area (Transylvania). *Acta Musei Sabesiensis*, *2*, 635-684.

966 Vremir, M., Kellner, A. W., Naish, D., & Dyke, G. J. (2013). A new azhdarchid pterosaur from
967 the Late Cretaceous of the Transylvanian Basin, Romania: implications for azhdarchid
968 diversity and distribution. *PLoS One*, *8*(1), e54268.

969 Vremir, M., Witton, M., Naish, D., Dyke, G., Brusatte, S. L., Norell, M., & Totoianu, R. (2015).
970 A medium-sized robust-necked azhdarchid pterosaur (Pterodactyloidea: Azhdarchidae)
971 from the Maastrichtian of Pui (Haţeg Basin, Transylvania, Romania). *American Museum*
972 *Novitates*, *2015*(3827), 1-16.

973 Vullo, R., Garcia, G., Godefroit, P., Cincotta, A., & Valentin, X. (2018). *Mistralazhdarcho*
974 *maggii*, gen. et sp. nov., a new azhdarchid pterosaur from the Upper Cretaceous of
975 southeastern France. *Journal of Vertebrate Paleontology*, *38*(4), 1-16.

976 Wang, X., Kellner, A. W., Jiang, S., & Cheng, X. (2012). New toothed flying reptile from Asia:
977 close similarities between early Cretaceous pterosaur faunas from China and
978 Brazil. *Naturwissenschaften*, *99*, 249-257.

979 Watabe, M., Suzuki, S., and Hayashibara Museum of Natural Sciences-Mongolian
980 Paleontological Center Joint Paleontological Expedition. (2000_. Report on the Japan-
981 Mongolia Joint Paleontological Expedition to the Gobi desert, 1994. *Hayashibara*
982 *Museum of Natural Sciences Research Bulletin* 1: 30–44.

983 Watabe, M., Tsogtbaatar, K., Suzuki, S., & Saneyoshi, M. (2010). Geology of dinosaur-fossil-
984 bearing localities (Jurassic and Cretaceous: Mesozoic) in the Gobi Desert: Results of the
985 HMNS-MPC Joint Paleontological Expedition. *Hayashibara Museum of Natural*
986 *Sciences Research Bulletin*, *3*(4), 41-118.

987 Watabe, M., Tsuihiji, T., Suzuki, S., & Tsogtbaatar, K. (2009). The first discovery of pterosaurs
988 from the Upper Cretaceous of Mongolia. *Acta Palaeontologica Polonica*, *54*(2), 231-242.

Wei, X., Pêgas, R. V., Shen, C., Guo, Y., Ma, W., Sun, D., & Zhou, X. (2021). Sinomacrops bondei, a new anurognathid pterosaur from the Jurassic of China and comments on the group. *PeerJ*, *9*, e11161.

Witton, M. P., & Habib, M. B. (2010). On the size and flight diversity of giant pterosaurs, the use of birds as pterosaur analogues and comments on pterosaur flightlessness. *PloS one*, *5*(11), e13982.

Witton, M. P., & Naish, D. (2008). A reappraisal of azhdarchid pterosaur functional morphology and paleoecology. *PLoS one*, *3*(5), e2271.

Zanno, L. E. (2010). A taxonomic and phylogenetic re-evaluation of Therizinosauria (Dinosauria: Maniraptora). *Journal of Systematic Palaeontology*, *8*(4), 503-543.

Zhou, X., Pêgas, R. V., Leal, M. E., & Bonde, N. (2019). *Nurhachius luei*, a new istiodactylid pterosaur (Pterosauria, Pterodactyloidea) from the Early Cretaceous Jiufotang Formation of Chaoyang City, Liaoning Province (China) and comments on the Istiodactylidae. *PeerJ*, *7*, e7688.

Zhou, X., Pêgas, R. V., Ma, W., Han, G., Jin, X., Leal, M. E., ... & Shen, C. (2021). A new darwinopteran pterosaur reveals arborealism and an opposed thumb. *Current Biology*, *31*(11), 2429-2436.

Zhou, X., Ikegami, N., Pêgas, R. V., Yoshinaga, T., Sato, T., Mukunoki, T., ... & Kobayashi, Y. (2024). Reassessment of an azhdarchid pterosaur specimen from the Mifune Group, Upper Cretaceous of Japan. *Cretaceous Research*, *167*, e106046.

Figures

Figure 1. Map of Mongolia. Highlighted are the aimags (provinces) of Dornogovi (East Gobi) and Ömnögovi (South Gobi) and the localities of Burkhant (1) and Bayshin Tsav (2).

Figure 2. MPC−Nd 100/302a, atlantoaxis of the holotype of *Gobiazhdarcho tsogtbaatari*. A, anterodorsal view; B, left lateral view; C, dorsal view; and D; E; F; respective schematic drawings. G, posterior view; H, right lateral view; and I, ventral view; and J; K; L, schematic

drawings. Abbreviations: ana, atlas neural arch; ai, atlas intercentrum; co, condyle; ct, cotyle; dy, diapophysis; ep, epipohysis; fo, fossa; nc, neural canal; ns, neural spine; po, postzygapophysis; poex, postexapophysis; pof, postzygapophyseal facet; pop, postzygapophyseal pedicle; py, parapophysis. Scale bar = 20 mm.

Figure 3. MPC−Nd 100/302b, cervical III of the holotype of *Gobiazhdarcho tsogtbaatari*. A, dorsal view; B, ventral view; C, anterior view; and D; E; F, respective schematic drawings. G, left lateral view; H, right lateral view; and I, posterior view; and J; K; L; schematic drawings. Abbreviations: adj.fo, adjacent foramen; co, condyle; ct, cotyle; dy, diapophysis; ipoel, interpostexapophyseal ridge; nc, neural canal; ns, neural spine; poex, postexapophysis; pop, postzygapophyseal pedicle; pop.b, postzygapophyseal pedicle base; poz, postzygapophysis; prex, preexapophysis; prf, prezygapophyseal facet; prp, prezygapophyseal pedicle; prz, prezygapohysis; ta.dis, taphonomic distortion; tr, transverse ridge; vlr, ventral longitudinal ridge; vtb, ventral tubercle. Scale bar = 20 mm.

Figure 4. MPC−Nd 100/302c, cervical VI of the holotype of *Gobiazhdarcho tsogtbaatari*. A, dorsal view; B, ventral view; C, posterior view; and D; E; F, respective schematic drawings. F, right lateral view; H, left lateral view; and I; J, schematic drawings. Abbreviations: adj.fo, adjacent foramen; co, condyle; ep, epipophyis; epk, epipophyseal keel; ipoel, interpostexapophyseal ridge; lf, lateral fossa; nc, neural canal; poex, postexapophysis; pof, postzygapophyseal facet; pop, postzygapophyseal pedicle; psp, posterior spinous process; tr, transverse ridge; vlr, ventral longitudinal ridge. Scale bar = 20 mm.

Figure 5. MPC−Nd 100/303, cervical VI of the holotype of *Tsogtopteryx mongoliensis*. A, anterior view; and B, schematic drawing; C, dorsal view; and D, schematic drawing; E, ventral view; and F, schematic drawing; G, left lateral view; and H, schematic drawing; right lateral view; and J, schematic drawing. Abbreviations: adj.fo, adjacent foramen; asp, anterior spinous process; ct, cotyle; cr, cervical rib; hy, hypapophysis; nc, neural canal; nr, neural ridge; poex.b, postexapophyseal base; pop.b, postzygapophyseal pedicle base; prf, prezygapophyseal facet; prk, prezygapophyseal keel; prp, prezygapophyseal pedicle; psp, posterior spinous process; tf, transverse foramen; tr, transverse ridge; vl.r, ventrolateral ridge; vertebrocostal sulcus. Scale bar = 10 mm.

Figure 6. Time-scaled strict consensus phylogenetic tree. Partial tree focused on the Azhdarchomorpha (the remaining of the tree is available in the Supplemental File 3). 1, Azhdarchomorpha; 2, Chaoyangopteridae.

Figure 7. Life restoration of the Bayanshiree azhdarchids. The coexistence between *Gobiazhdarcho tsogtbaatari* and *Tsogtopteryx mongoliensis* in the Bayanshiree paleoenvironment, with a group of *Gobihadros mongoliensis* nearby. Artwork by Zhao Chuang.

Tables

Table 1. Phylogenetic nomenclature.

Supplemental Files

Supplemental File 1. Mesquite file. A nexus-format file for Mesquite, containing the phylogenetic data matrix.

Supplemental File 2. TNT file for the phylogenetic analysis.

Supplemental File 3. Supplemental text. A text file containing details on the wingspan estimates and the complete strict consensus tree.

Table 1(on next page)

Phylogenetic nomenclature.

Reference phylogeny: this work. Original definitional authors and Regnum codes are given between square brackets. Authors and Regnum codes of unrestricted emended definitions are given between curly braces. See the main text for further comments on the diagnoses and compositions of azhdarchid clades.

Clade	Nominal and definitional authors, and Regnum code	Definition	Composition and remarks
Azhdarchoidea	Unwin 1995 [Andres 2021], [355].	Min ∇ *Tapejara wellnhoferi* Kellner 1989 & *Quetzalcoatlus northropi* Lawson 1975.	Includes the sister-taxa Tapejaromorpha and Azhdarchomorpha.
Azhdarchomorpha	Pêgas *et al.* 2021 [Pêgas *et al.* 2021], [574].	Max ∇*Azhdarcho lancicollis* Nessov 1984 ~ *Thalassodromeus sethi* Kellner & Campos 2002 & *Tapejara wellnhoferi* Kellner 1989.	Includes *Keresdrakon*, Chaoyangopteridae, and Azhdarchiformes.
Azhdarchiformes	Andres 2021 [Andres 2021], [771].	Max ∇ *Quetzalcoatlus northropi* Lawson 1975 ~ *Chaoyangopterus zhangi* Wang & Zhou 2003.	Includes Alanqidae and Azhdarchidae.
Alanqidae	Pêgas *et al.* 2021 [Pêgas *et al.* 2021], [576].	Max ∇ *Alanqa saharica* Ibrahim *et al.* 2010 ~ *Chaoyangopterus zhangi* Wang & Zhou 2003 & *Azhdarcho lancicollis* Nessov 1984.	Includes *Alanqa*, *Argentinadraco*, *Leptostomia*, and *Xericeps*.
Azhdarchidae	Padian 1986 {this work}, {1043}	Min ∇ *Azhdarcho lancicollis* Nessov 1984, *Phosphatodraco mauritanicus* Pereda-Suberbiola *et al.* 2003, *Zhejiangopterus linhaiensis* Cai & Wei 1994, & *Quetzalcoatlus northropi* Lawson 1975.	See main text for a detailed protologue including remarks on its composition and conceptualization.
Phosphatodraconia (new clade name)	This work [this work], [1044].	Max ∇ *Phosphatodraco mauritanicus* Pereda-Suberbiola *et al.* 2003 ~ *Azhdarcho lancicollis* Nessov 1984, *Zhejiangopterus linhaiensis* Cai & Wei 1994 & *Quetzalcoatlus northropi* Lawson 1975.	Includes *Aralazhdarcho*, *Eurazhdarcho*, *Phosphatodraco*, and *Wellnhopterus*.
Quetzalcoatlida (new clade name)	This work [this work], [1045].	∇ apomorphy piriform/clithridiate neural canal opening [*Quetzalcoatlus lawsoni* Andres & Langston 2021].	Includes Hatzegopterygia and Quetzalcoatlini.
Hatzegopterygia (new clade name)	This work [this work], [1046].	Max ∇ *Hatzegopteryx thambema* Buffetaut *et al.* 2002 ~ *Quetzalcoatlus northropi* Lawson 1975.	Includes *Albadraco*, *Cryodrakon*, *Hatzegopteryx*, the Pui azhdarchid, and *Tsogtopteryx*.
Quetzalcoatlini (new clade name)	This work [this work], [1047].	Max ∇ *Quetzalcoatlus northropi* Lawson 1975 ~ *Hatzegopteryx thambema* Buffetaut *et al.* 2002.	Includes *Arambourgiania*, *Gobiazhdarcho*, *Nipponopterus*, *Quetzalcoatlus*, and *Thanatosdrakon*.

Table 1. Phylogenetic nomenclature. Reference phylogeny: this work. Original definitional authors and Regnum codes are given between square brackets. Authors and Regnum codes of unrestricted emended definitions are given between curly braces. See the main text for further comments on the diagnoses and compositions of azhdarchid clades.

Figure 1

Map of Mongolia.

Highlighted are the aimags (provinces) of Dornogovi (East Gobi) and Ömnögovi (South Gobi) and the localities of Burkhant (1) and Bayshin Tsav (2).

Figure 2

MPC−Nd 100/302a, atlantoaxis of the holotype of *Gobiazhdarcho tsogtbaatari*.

A, anterodorsal view; B, left lateral view; C, dorsal view; and D; E; F; respective schematic drawings. G, posterior view; H, right lateral view; and I, ventral view; and J; K; L, schematic drawings. Abbreviations: ana, atlas neural arch; ai, atlas intercentrum; co, condyle; ct, cotyle; dy, diapophysis; ep, epipohysis; fo, fossa; nc, neural canal; ns, neural spine; po, postzygapophysis; poex, postexapophysis; pof, postzygapophyseal facet; pop, postzygapophyseal pedicle; py, parapophysis. Scale bar = 20 mm.

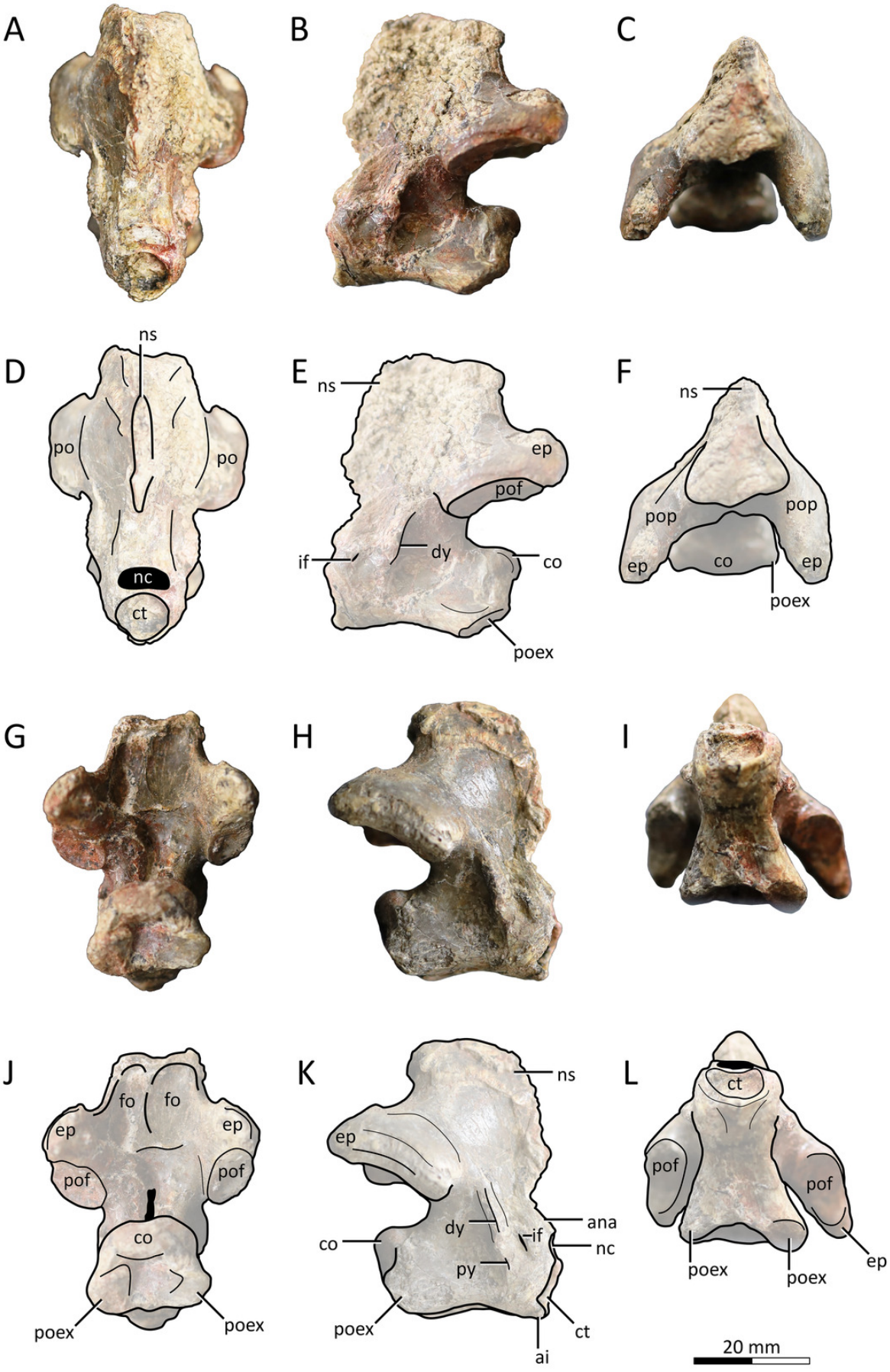
A
B
C
D
ns
po
po
nc
ct
E
ns
ep
pof
if
dy
co
poex
F
ns
pop
pop
ep
co
ep
poex
G
H
I
J
fo
fo
ep
ep
pof
pof
co
poex
poex
K
ns
ep
dy
ana
if
nc
co
py
poex
ct
ai
L
ct
pof
pof
poex
poex
ep
20 mm

Figure 3

MPC−Nd 100/302b, cervical III of the holotype of *Gobiazhdarcho tsogtbaatari*.

A, dorsal view; B, ventral view; C, anterior view; and D; E; F, respective schematic drawings. G, left lateral view; H, right lateral view; and I, posterior view; and J; K; L; schematic drawings. Abbreviations: adj.fo, adjacent foramen; co, condyle; ct, cotyle; dy, diapophysis; ipoel, interpostexapophyseal ridge; nc, neural canal; ns, neural spine; poex, postexapophysis; pop, postzygapophyseal pedicle; pop.b, postzygapophyseal pedicle base; poz, postzygapophysis; prex, preexapophysis; prf, prezygapophyseal facet; prp, prezygapophyseal pedicle; prz, prezygapohysis; ta.dis, taphonomic distortion; tr, transverse ridge; vlr, ventral longitudinal ridge; vtb, ventral tubercle. Scale bar = 20 mm.

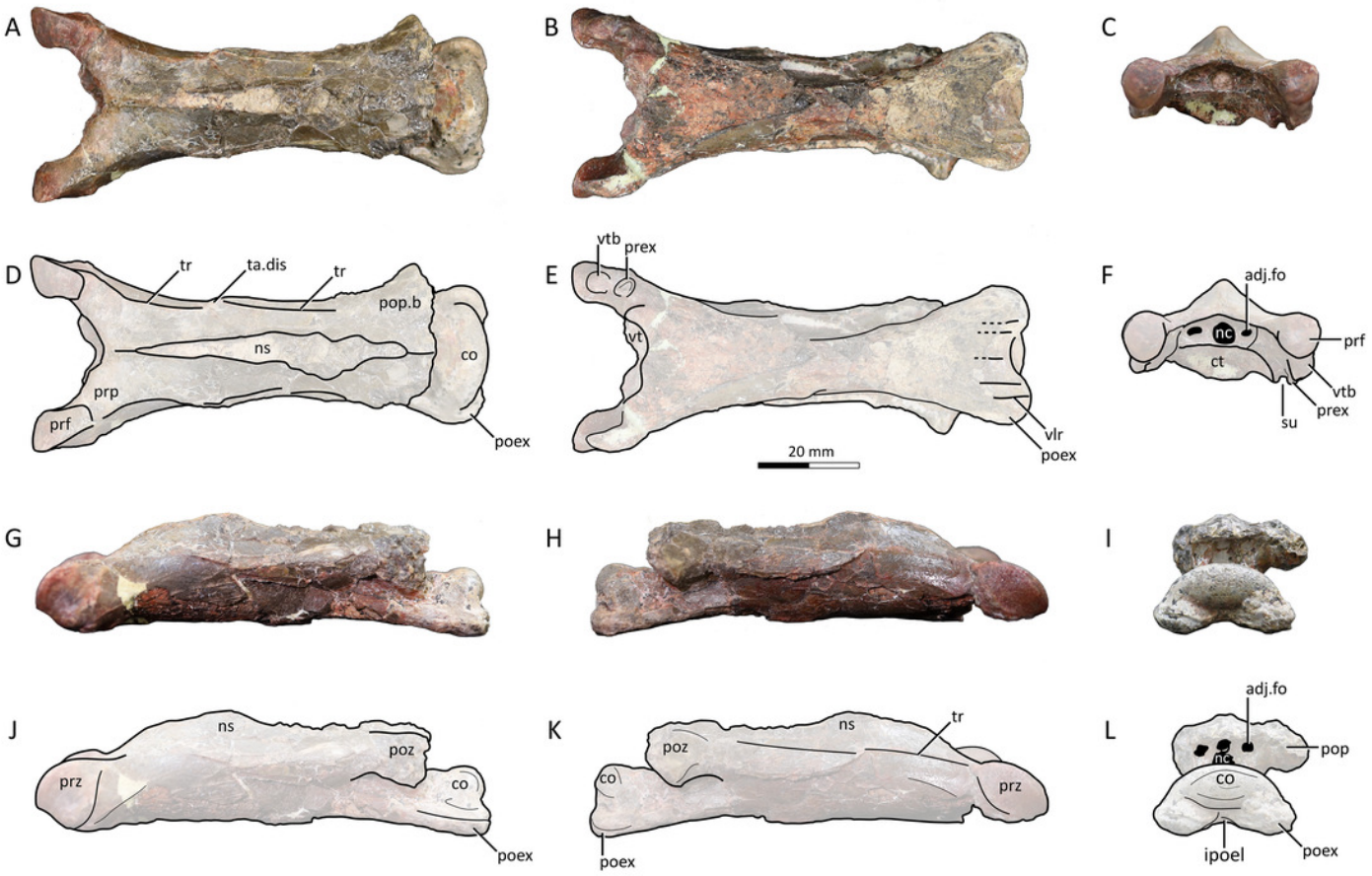

Figure 4

MPC−Nd 100/302c, cervical VI of the holotype of *Gobiazhdarcho tsogtbaatari*.

A, dorsal view; B, ventral view; C, posterior view; and D; E; F, respective schematic drawings. F, right lateral view; H, left lateral view; and I; J, schematic drawings. Abbreviations: adj.fo, adjacent foramen; co, condyle; ep, epipophyis; epk, epipophyseal keel; ipoel, interpostexapophyseal ridge; lf, lateral fossa; nc, neural canal; poex, postexapophysis; pof, postzygapophyseal facet; pop, postzygapophyseal pedicle; psp, posterior spinous process; tr, transverse ridge; vlr, ventral longitudinal ridge. Scale bar = 20 mm.

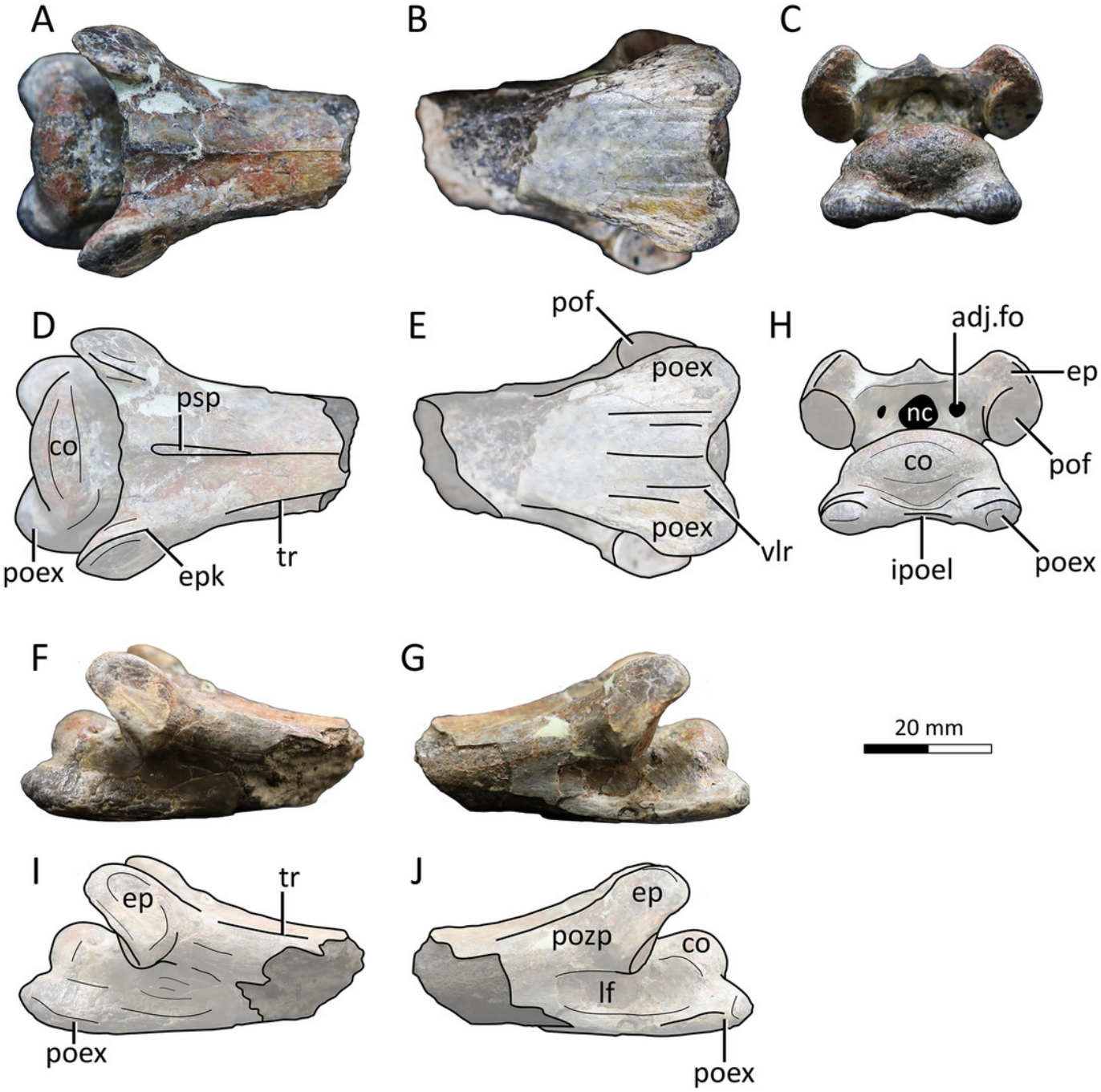
A
B
C
D
psp
co
poex
epk
tr
E
pof
poex
poex
vlr
H
adj.fo
ep
nc
co
pof
ipoel
poex
F
G
20 mm
I
ep
tr
poex
J
ep
pozp
co
lf
poex

Figure 5

MPC−Nd 100/303, cervical VI of the holotype of *Tsogtopteryx mongoliensis*.

A, anterior view; and B, schematic drawing; C, dorsal view; and D, schematic drawing; E, ventral view; and F, schematic drawing; G, left lateral view; and H, schematic drawing; right lateral view; and J, schematic drawing. Abbreviations: adj.fo, adjacent foramen; asp, anterior spinous process; ct, cotyle; cr, cervical rib; hy, hypapophysis; nc, neural canal; nr, neural ridge; poex.b, postexapophyseal base; pop.b, postzygapophyseal pedicle base; prf, prezygapophyseal facet; prk, prezygapophyseal keel; prp, prezygapophyseal pedicle; psp, posterior spinous process; tf, transverse foramen; tr, transverse ridge; vl.r, ventrolateral ridge; vertebrocostal sulcus. Scale bar = 10 mm.

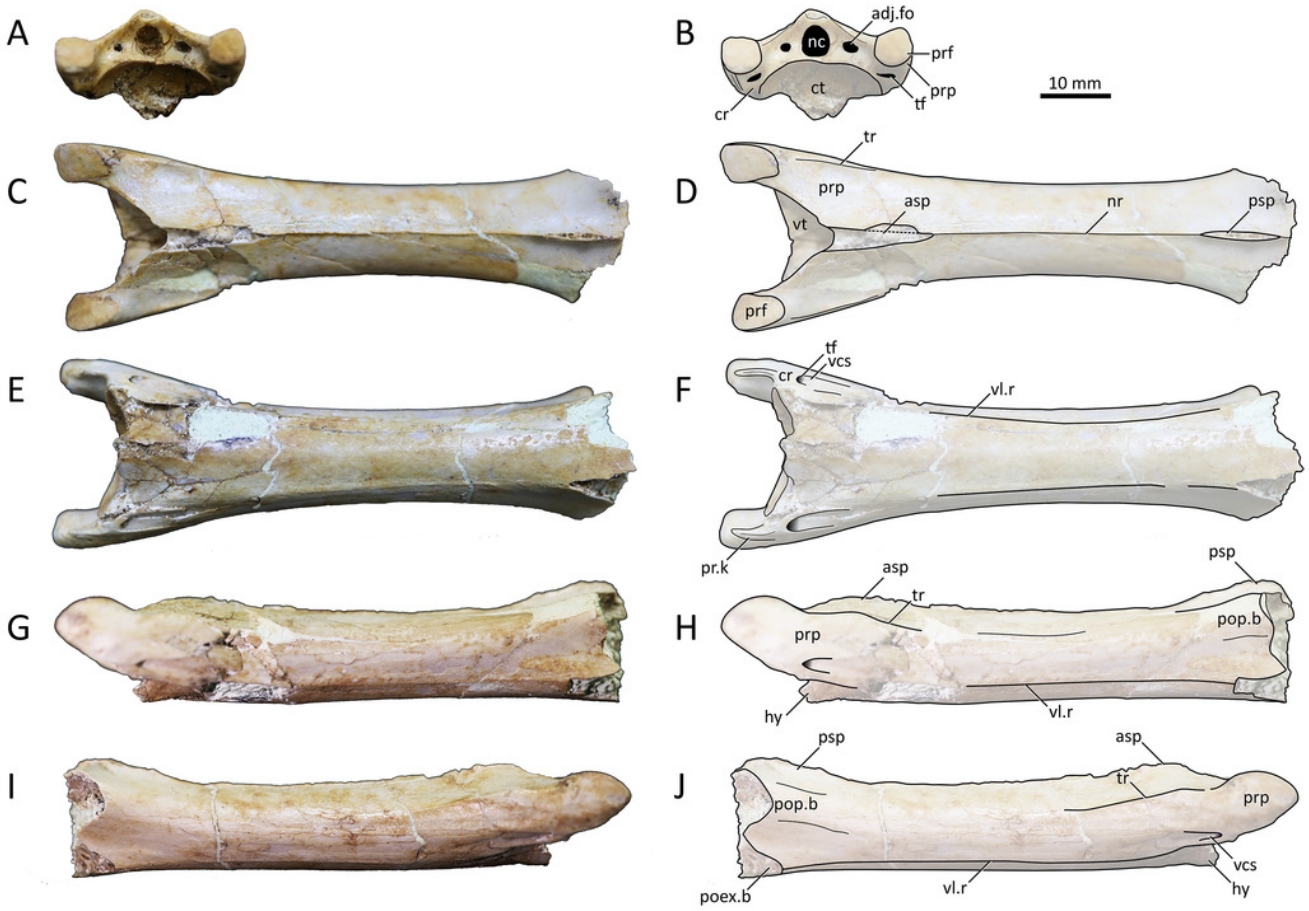

Figure 6

Time-scaled strict consensus phylogenetic tree.

Partial tree focused on the Azhdarchomorpha (the remaining of the tree is available in the Supplemental File 3) . 1, Azhdarchomorpha; 2, Chaoyangopteridae.

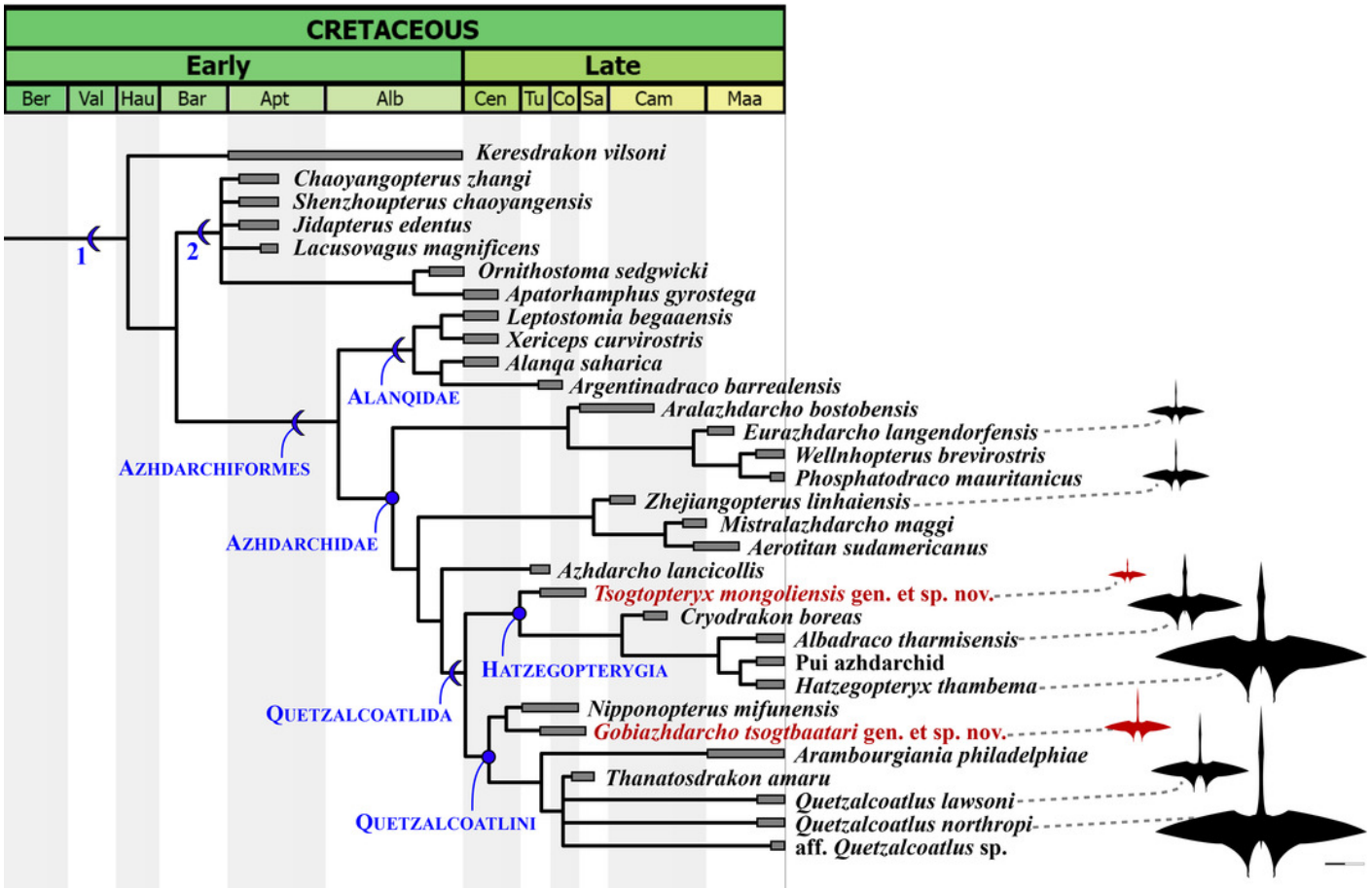

Figure 7

Life restoration of the Bayanshiree azhdarchids.

The coexistence between *Gobiazhdarcho tsogtbaatari* and *Tsogtopteryx mongoliensis* in the Bayanshiree paleoenvironment, with a group of *Gobihadros mongoliensis* nearby. Artwork by Zhao Chuang.